Development of Nanocomposite Membranes Based on PVA (Polyvinyl Alcohol) and Functionalized Nano Cellulose for Biogas Upgrading

By

Saleem Ahmad

School of Chemical and Materials Engineering

National University of Sciences and Technology

2020

Development of Nanocomposite Membranes Based on PVA (Polyvinyl Alcohol) and Functionalized Nano Cellulose for Biogas Upgrading

Name: Saleem Ahmad

Registration No: 00000206974

This thesis is submitted as partial fulfillment of the requirements for the degree of

MS in (Chemical Engineering)

Supervisor Name: Dr. Zaib Jahan

Co-Supervisor: Dr. Muhammad Bilal Khan Niazi

School of Chemical and Materials Engineering (SCME)

National University of Sciences and Technology (NUST)

H-12 Islamabad, Pakistan

january, 2020

Dedication

Devoted to my Dearest Guardians and Kin

Acknowledgments

Knowledge is limited to praise ALMIGHTY ALLAH, the Beneficent and the Merciful, who is the source of knowledge and whose blessing is the cherish of my thoughts. Peace and blessing of ALLAH on our beloved PROPHET HAZRAT MUHAMMAD (PBUH), the greatest social reformer, that is the cause of the creation of the universe and the forever source of knowledge and guidance for mankind.

I would like to express my sincere gratitude to my project supervisor Dr. Zaib Jahan (Chemical Engineering Department, SCME-NUST) for her support in my master's research work, for his motivation and patience. She helped me in my research and writing of the thesis.

My deepest gratitude to my supervisor, Dr. Zaib Jahan, to whom I cannot thank enough for her dedication, help, and support throughout my work. I am deeply thankful to her for believing in me. She was always there when I needed any kind of assistance.

I am deeply thankful to my co-supervisor, Dr. Muhammad Bilal Khan Niazi, and my Guidance and Exam Committee (GEC) members, Dr. Arshad Hussain and Dr. Imran Ullah Niazi, for their help and support on moral and material grounds. Their motivation kept me going and their help assisted me to complete this project.

I would like to thank the lab staff for their assistance in carrying out necessary testing and characterization techniques.

I am thankful to my family for their prayers, love and support me throughout my life. At last, I would like to thank all lab staff members of SCME, for their support during lab work.

Abstract

Globally, the consumption of energy has increased compared to the average rate of growth**.** To fulfill the world energy requirement, the demand for fuels has also increased. From initial decade fossil fuel was used as a major source of energy production. These sources of fossil fuels are depleting very rapidly. So, the world is now moving toward renewable energy resources. Biogas is one of the most suitable options to use as a renewable energy source. It is required to upgrade the raw biogas to fulfill high quality energy and demands. It can be upgraded by removing CO_2 from CH_4. After upgradation of biogas, CH_4 contents in biogas has increased up to 95%. This upgraded biogas can be used in various applications such as fuel of vehicles, in power grid stations and for domestic use.

For upgrading biogas, it is essential to follow such process of upgrading which has high efficiency and low energy-consumption. Membrane technology is one of the green and emerging technology. As compared to commercially available technology, it has many advantages over other state of the art technologies. Permeability and selectivity are the major parameters to determine the performance of membranes. In order to compete with other technologies available in the market, it required to have high CO_2 permeance and high selectivity of membranes.

Different type of materials is used for membrane fabrication like organic (polymeric), inorganic, ceramics, and ionic liquid. Polymeric membranes are most suitable option to be used as commercial membranes because of its easy fabrication, low cost and high separation performance. Facilitated transport membranes (FTMs) are one of the innovative approaches for CO_2 separation with high CO_2 permeance and high selectivity. In these membranes, additives are embedded in polymeric matrixes to facilitate the CO_2 transport through solution diffusion mechanism.

In most FTMs water/moisture act as carrier that enhances the CO_2 transportation through membrane. Therefore, the performance of FTMs can be improved by increasing its moisture uptake ability. In this research work, novel FTM (nanocomposite membrane) was developed based on polyvinyl alcohol (PVA) as a basic polymer with aminated

cellulose nanocrystal (Am-CNC) as a filler. CNC were first functionalized and then added to PVA matrix.

The casted membranes were characterized by using X-ray Diffraction (XRD), Fourier Transform Infra-red (FTIR) and Scanning Electron Microscopy (SEM) as supporting techniques. XRD technique was used to investigate the crystalline nature of nanocomposite membranes and crystallinity of CNC and Am-CNC while FTIR technique was used to investigate the amine functional group attachment to the CNC and in nanocomposite membrane while SEM was used to observed the surface morphology and cross sectional of nanocomposite membrane.

Permeance testing was used to observed the permeability and selectivity performance of nanocomposite membranes for CO_2/CH_4. It was observed that by increasing the concentration of Am-CNC, the thickness of selective dense layer also increased that result in decrease in permeability. However, the moisture uptake ability was also investigated that shows maximum value up to addition of 1 wt.% of Am-CNC.

The permeance and selectivity of CO_2 and CH_4 across membranes against high feed pressures i.e. 5, 10, 15 bar was investigated. It was noticed that by increasing feed pressure both the permeance and selectivity of CO_2 and CH_4 was decreased. However, the values for CO_2 permeance are comparably high as compared to that for CH_4. The best result for CO_2 permeance and selectivity was observed for 1 wt.% Am-CNC/PVA based nanocomposite membrane.

This research work consists of single gas testing however, the results support that membranes has high affinity towards CO_2 as compared to CH_4.The resultant membranes can be used for upgrading the biogas system as a potential technology in future.

Table of Contents

List of Figures

List of Tables

Abbreviation

VOCs	Volatile Organic Compound
PSA	Pressure Swing Adsorption
PVP	Polyvinylpyrrolidone
PSF	Poly Sulphone
PVA	Polyvinyl Alcohol
PVAm	Polyvinyl Amine
PU	Poly Urethane
FTM	Facilitated Transport Membrane
KBr	Potassium Bromide
MOFs	Metal Organic Frame Work
CNTs	Carbon Nanotubes
CNF	Cellulose Nanofibers
CNC	Cellulose Nanocrystal
PVDF	Polyvinylidene Difluoride
PES	Polyether Sulfone
MMMs	Mixed Matrix Membranes
FSCs	Fixed-site Carrier Membranes
FTIR	Fourier Transform Infra-Red

XRD	X-ray Diffraction
SEM	Scanning Electron Microscope
DOS	Degree of Swelling
STP	Standard Temperature and Pressure
RH	Relative Humidity

Chapter 1

Introduction

1.1 Back Ground

Globally, the consumption of energy increased nearly twice in 2018 as compared to the average rate of growth in 2010 [1]. International environmental agency published a report "titled" global energy and CO_2 status in year 2018. According to this report, the countries which are the leading producer, as well as leading consumer of world energy, are; United States, Russia, and China. They produced about 30% of world energy and consumed about 40% of world energy. To fulfill the world energy requirement, the demand for fuels increased [1]. From the initial decade, fossil fuel is used as a major source for energy production. Oil demand increased approximately by 1.5% in 2018, in which the US was a major consumer led by China, India, and Europe. Natural gas consumption, in 2018, was increased approximately by 4.9% in which US was a major consumer led by china. Coal consumption is increased proximately by .8% which is quite less than in previous years (2001-2011) demand which is approximately 4.7% [1]. The demand and supply of fossil fuel depend on their reservoirs and supply roots. About 80% of world oil reservoirs are in ten countries, similarly half of world natural gas stack are in three countries, while coal 80% world stock are in six countries. Some of these countries exercise their power to restrict the supply or affect the prices of fossil fuels [2].

Fossil fuels are nonrenewable resources, so they will be deleted. The approximate depletion times for coal, gas, and oil are 108, 39 and 36 years respectively. So the only available reserves will be coal in 2114. It will be only fossil fuel after 2042. Other challenges concern to fossil fuel is environmental, geopolitical, military and fluctuating prices. These concerns will create unsustainability for human societies [2]. To resolve these all concerns related to fossil fuel the world is moving toward renewable and sustainable energy resources. Sustainable energy resources are defined as the resources which are equality available for all peoples and also preserve on earth for the future generation. Massachusetts Institute of Technology (MIT) released a press "titled" sustainable energy: Choosing among the options. According to which renewable sources

of energy withstand themselves naturally without depleting on earth. Some of their sources are; hydropower, wind, tidal, geothermal, solar and bioenergy [3]. The contribution of renewable energy resources in world energy demand will be approximately 48% up to 2040. **Table 1** shows the scenario of global renewable energy by 2040.

Table 1: Renewable Energy Consumption [4]

	2001	**2010**	**2020**	**2030**	**2040**
Total consumption (Kteo)	10,039	10,551	11,427	12,352	13,315
Biomass	1083	1315	1793	2486	3274
Large hydro	22.9	268	311	345	359
Geothermal	43.4	87	187	334	495
Small hydro	9.6	20	50	107	190
Wind	4.8	45	267	543	689
Solar thermal	4.2	14	67	243	879
Photovoltaic	0.2	3	25	222	783
Solar electricity	0.2	0.5	4	17	69
Tidal	0.04	0.2	0.5	4	21
Total RES	1365.7	1745.6	2964.7	4291	6352
Renewable source contribution (%)	13.7	16.8	23.7	34.9	47.8

It can be seen from table 1 that biomass raw material is abundantly available as compared to other renewable resources. The other resources like solar energy depend on the availability of sunlight, wind energy depends on wind and tidal energy depends on ocean tides, etc. Biogas production through anaerobic digestion of biomass has significant advantages over other bio energies. Biogas production technology has been considered as the most energy-efficient technology for bioenergy production. Several raw materials and different technologies are used for biogas production. It can be used at the domestic level for burning. The raw material for biogas contains organic waste from houses and food industries, energy crops, agricultural waste, and animal manure [5].

1.2 Biogas

Biogas is one of modern renewable energy produced by Anaerobic digestion, a series of biological processes, in which micro-organisms digest the organic waste material in sealed containers to produce biogas, which has a mixture of CH_4, CO_2, and other gases. Organic materials are; industrial sewage, municipal waste, agricultural matter, Livestock manures, commercial and domestic food waste, and some plants can be also treated to get energy [6]. Biogas can be used in both scales; small scale for household's purpose; directly burn-in domestic stoves for cooking or used in gas lamps, for lighting and large scale for the industrial purpose; boiler heating to generation steam, internal and external heat engine for electricity. While the organic material such as nitrogen, potash, and phosphate, which left in a digester after digestion are used as a fertilizer in agricultural fields [6]. Figure 1 shows the process flow diagram for biogas production and utilization;

Figure 1: Process Flow Diagram for Biogas Production and Utilization [7]

Table 2: Composition of Raw Biogas [8]

Serial No.	Name of component	Composition (%)
1	CH_4	45-75
2	CO_2	25-55
3	H_2O	4-10
4	N_2	2-3
5	O_2	1-2
6	H_2S	1-2
7	VOCs	0.021
8	Siloxanes	0.004
9	Ammonia	Traces

There are wide applications of biogas technologies around the world. The biogas industries can be analyzed in the following three categories; biogas based micro digesters, electricity-generating scale digesters, bio methane-producing scale digesters [8].

In developing counties, biogas is produced in villages by micro digester, which is used for domestic purposes e.g. for cooking, lighting. World biogas association published a report "titled" Global potential of bio gas in 2018. According to this report, on the global level, there are currently around 49.5 million of micro-scale digesters operating, in which approximately 41.5 million operating in China, and about 4.8 million in India [9]. While the rest of approximately 700,500 biogas plants are installed in the rest of Asia, Africa, and South America [9]. On scale level biogas digester used for electricity generation, it is well-established technology that is widely implemented around the world. In china approximately 110,450 biogas plants are operating, in which approximately 6,974 are at large scale, about 17,785 biogas plants are installed in Europe with 10.6 GW capacity. Following are the distribution of biogas plants in Europe countries; Germany has 10,972 plants, Italy has 1,656, France has 743, Switzerland has 633 and UK has 2,200 biogas plants [10]. USA has 2203 biogas digesters with capacity of 978 MW, India have capacity of 300MW, Canada has about 181 plants with capacity of 197 MW. Based on the above calculation there are approximately 132,010 all size biogas plants are operating in the world [11].

1.3 Biogas Upgrading:

In biogas, presence of CO_2 in large amount caused to reduce the calorific value of biogas which effect the heating quality of biogas. The energy content of biogas described by term LCV (lower calorific value), which is 50.5 MJ/kg-CH_4 or 36.5 MJ/m^3-CH_4 at STP condition. When biogas have CH_4 contents about (55-65%), its LCV is around (21-25 MJ/m^3-biogas). Therefore, it is necessary to improve the quality of biogas up to (95% of CH_4 contents) by removing these undesired components which affect the quality of biogas e.g. CO_2 and H_2O decrease the LCV of biogas, H_2S and NH_3 are very toxic and corrosive which effect the combined heat and power unit and metal parts by generating SO_2 during combustion and siloxanes generate silicone oxides during combustion which has sticky residues, it deposits on engines and valves of biogas combustion plant and cause malfunction [9]. There are two types of treatments needed to improve the quality of biogas, in which one is known as biogas cleaning and second is known as biogas upgrading [12]. Figure 2 give flow diagram for biogas upgrading;

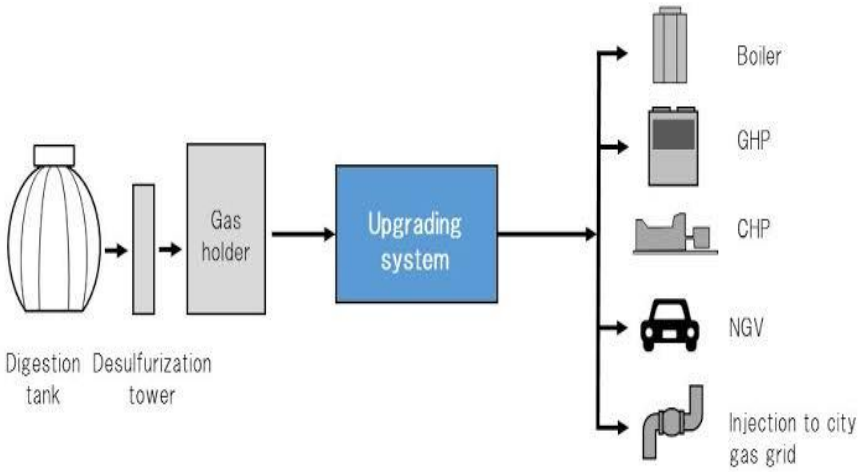

Figure 2 : Flow Diagram for Biogas Upgrading [13]

1.3.1 Biogas Pretreatment

In biogas cleaning, the harmful and toxic compounds like H_2S, Si, VOCs, siloxanes, CO, H_2O, and NH_3 are removed. The techniques used for H_2S removal; Absorption in liquid-like caustic soda solution or water, absorption on a solid surface like activated carbon or iron oxide or biological conversion in which sulfur compounds are converted into elemental sulfur [14]. Water vapors in biogas may condensate in pipelines cause corrosion, water can be removed by absorption, adsorption, cooling, and compression, in which water is condensate by increasing pressure and decreasing temperature i.e. cryogenic condensation [15].

1.3.2 Upgrading Technique

Biogas upgrading is defined as; to increase the energy intensity of biogas by removing carbon dioxide, since to improve methane concentration. The techniques used for biogas upgrading are; Pressure Swing Adsorption (PSA), in this technique mainly CO_2 are removed. Under high pressure, the raw biogas is observed on absorbent material, which are; carbon molecular sieve activated carbon, zeolite and other materials having the high surface area. The main principle for this technique is; CO_2 is absorbed in the absorbent surface under high pressure, while, released it by decreasing that pressure [16]. In absorption technique the counter flow of raw biogas and liquid in a column filled with plastic packing is conduct. The main principle behind it is, CO_2 is more soluble then CH_4, the liquid leaving the column have high concentration of CO_2 while gas leaving has high CH_4 concentration. Scrubbing techniques also used for biogas upgrading. On bases of absorbent materials scrubbing is; water scrubbing, in which carbon dioxide solubility in water is higher than methane so carbon dioxide will have dissolved at higher extent than methane at lower temperatures. In chemical scrubbing, amine-based solution is used, CO_2 absorbed in liquid and chemically react with the amine in a liquid. The reaction is selective so no effect on CH_4. The liquid in which CO_2 is absorbed is recycled by heating [15]. The processes discussed above are widely used for CO_2 separation from biogas but there are some issues related to these processes; highly energy-intensive, more expensive and environment-related issues.

Therefore, the center of attention has been diverted to introduce such a process for biogas upgrading, which is more energy-efficient, less expensive, and environment-friendly. So, a lot of research has been conducted to investigate such processes. From this research, it has been found that the membrane-based technologies for biogas upgrading are one of the competitive processes, which fulfill all these above-given criteria like membranes-based technologies that are much energy-efficient than other conventional methods. It only needs about 50% less energy than other processes, it can replace other techniques because of its easy fabrication, easily integrate within the existing industries setup and finally easy to scale up [17].

1.4 Gas Separation Membrane

The main focus of the research area is membrane technology for gas separation because it provides the most effective and reliable way to resolve the problem related to energy, cost, and environment. According to Benny D. Freeman, "the role of the membrane is very important in the field of environment and energy processes like hydrogen and methane purification".

Main processes for gas separation are the following:

- Nitrogen and oxygen separation from air
- Hydrogen removal from different resources like methane and nitrogen
- Increasing the concentration of methane in biogas by separating other gas components like CO_2, N_2, H_2S
- Purification of natural gas by separating CO_2 and H_2S

These are some processes for which membrane technology shows compatible results as compared to the other one. There are some criteria in favor of membrane which are explained by Baldus and Tillman, it should be fulfilled before using the membrane for gas separation.

- When the purity of moderate quality is needed
- When important products are obtained after separation like methane
- When the feed gas must be free from all impurities like H_2S which affect the surface of the membrane and reduced its function

- When the selectivity of the membrane must be high for the desired component as compared to the other one
- When the feed gas interring to the membrane is at the desired pressure and the pressure at the concentrate side needed to be high [17]

The organic or inorganic materials which are used in membrane fabrication should have some specific properties, like their physical and chemical properties, which have the ability to separate different desired components from the mixture of gases successfully. These properties include their mechanical stability and chemical stability, which means that membrane materials have enough ability to stay in functional condition for a long time. Following factors which affect the membrane ability to separate gases:

- Materials used in the fabrication of membranes, which affect properties like permeability and selectivity of the membrane.
- Surface and cross-sectional morphology of membrane, which affects the permeance of the membrane.
- Membrane modification in Module like hollow fiber, plate, and frame, spiral wound, flat sheet for commercial-scale usage [18].

There are two basic parameters that defined the performance of gas separating membrane; permeability and selectivity.

Permeability is defined as the "Components permeation rate through membrane".

$$P = \frac{Q.l}{A.\Delta p}$$

Where

Q = flow rate

L = membrane thickness

A = area of membrane

Δp = pressure difference

It depends on two major factors:

- Thermodynamic factor, which deals with components separation from the gas mixture after passing through the membrane.
- Kinetic factor, which deals with the diffusion of the components through a dense layer of the membrane.

While selectivity is defined as "the ability of the membrane to how much preferentially it permeates one component as compared to other from a mixture".

$$\alpha = \frac{p_{CO_2}}{p_{CH_4}}$$

it is important because it relates to better and pure product recoveries. If such a membrane which have both higher permeability and selectivity is being fabricated then it will make a membrane technology one of its enormous growth [19].

In the fabrication of gas separation membranes, the selection of material is an important step. The choice of material for membrane fabrication depends on their physical and chemical properties, their effective interaction with the components of gases which are desired to separate from the mixture. If membrane materials have some type of functional groups in their chains, then it develops affinity to only some particular component of gas, so that component will separate from the mixture, which improves the separating ability of membrane. Some of membrane fabricating material are polymers, glass, metals and ceramic [20, 21].

1.4.1 The Basic Principle for Membrane Separation

The basic principle of the membrane is "A semipermeable layer which has the ability to selectively separate or pass one of the component through it from a mixture". The main driving force for the gas separation is "the difference of chemical potential and the partial pressure difference on both sides of membrane". **Figure 3** defining the separation principle for membrane [22].

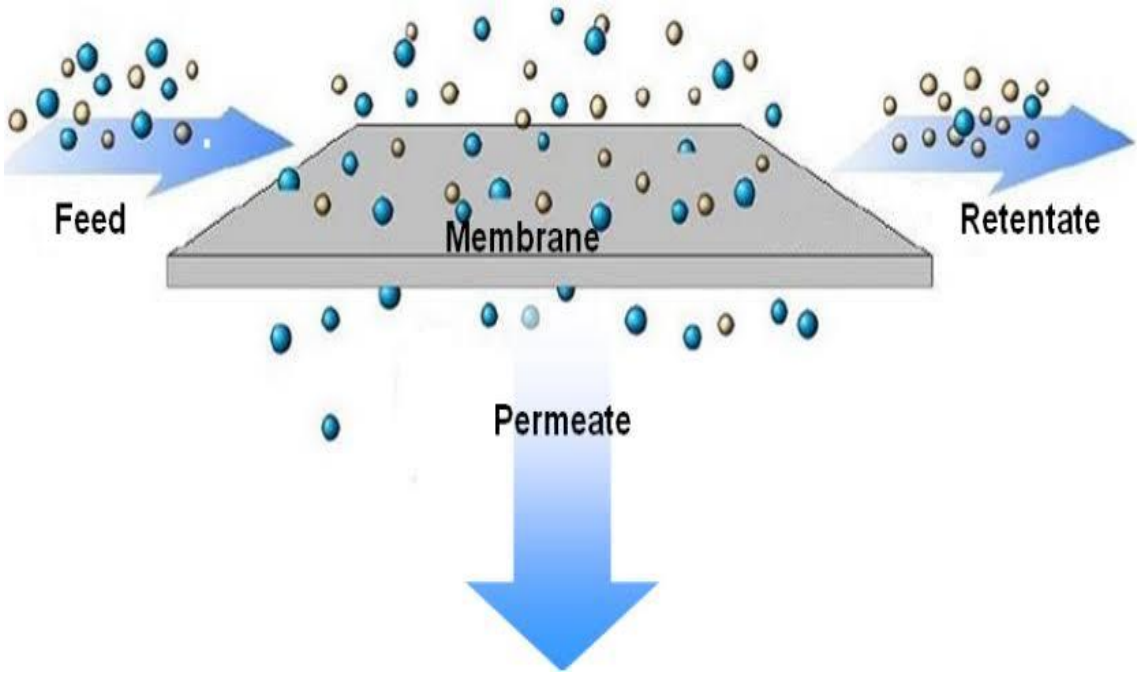

Figure 3: Gas Separation Principle [22]

There are different mechanisms used by membrane for gas separation which is given as;

- Adsorption-diffusion mechanism
- Solution-diffusion mechanism
- Knudsen-diffusion mechanism
- Capillary condensation
- Molecular sieve mechanism.

These mechanisms depend on the type of gas to separate and type of membrane to be used for separation. Some of these mechanisms are related to **figure 4**.

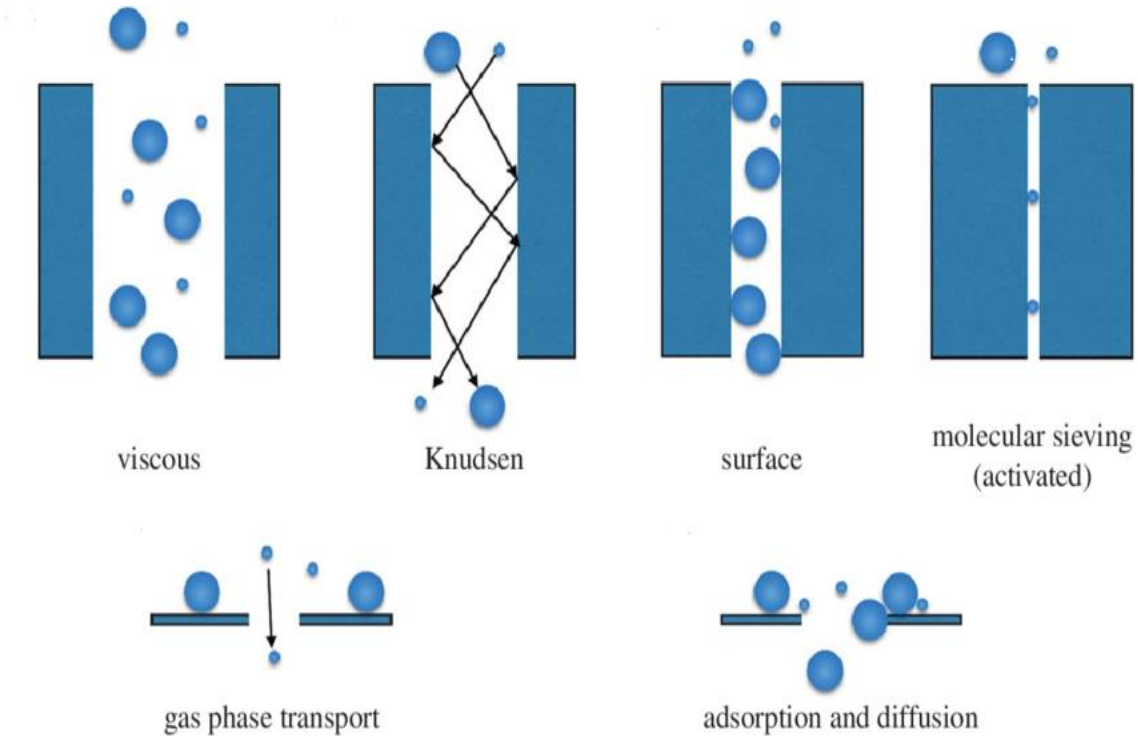

Figure 4: Different Mechanisms Used in the Membrane for Gas Separation [23]

1.4.2. Basic Models for Separation Mechanism

There are two basic models which described the permeation and separation mechanism;

- Solution diffusion model
- Pore flow model

1.4.2.1 Solution Diffusion Model

In this model, the components which want to permeate through the membrane, first dissolve in the polymer of the membrane and then due to the concentration gradient that component diffuses across the membrane. So, the separation based on the solubility of components in the polymer of the membrane and their diffusion rates across the membrane [24]. These phenomena of movement of molecules from higher concentration towards lower concentration were first studied by Fick's in 1855 and called as Fick's law [25]:

$$Ji' = -Di'.(\frac{dci'}{dx'})$$

Where,

Ji'= flux(g/cm^{2}s)

dci'/dx' =concentration gradient

Di' = diffusion coefficient (cm^2/s)

In above equation, the diffusion coefficient is for the mobility rate of a single molecule, while the negative sign is for the motion of molecules from higher concentration to lower concentration region. In this model where the Fick's law is applicable, the pores have no defined shape and size but they are conceder as a space between the chain of the polymer [25]. The pore flow and solution diffusion model are explained in **figure 5**:

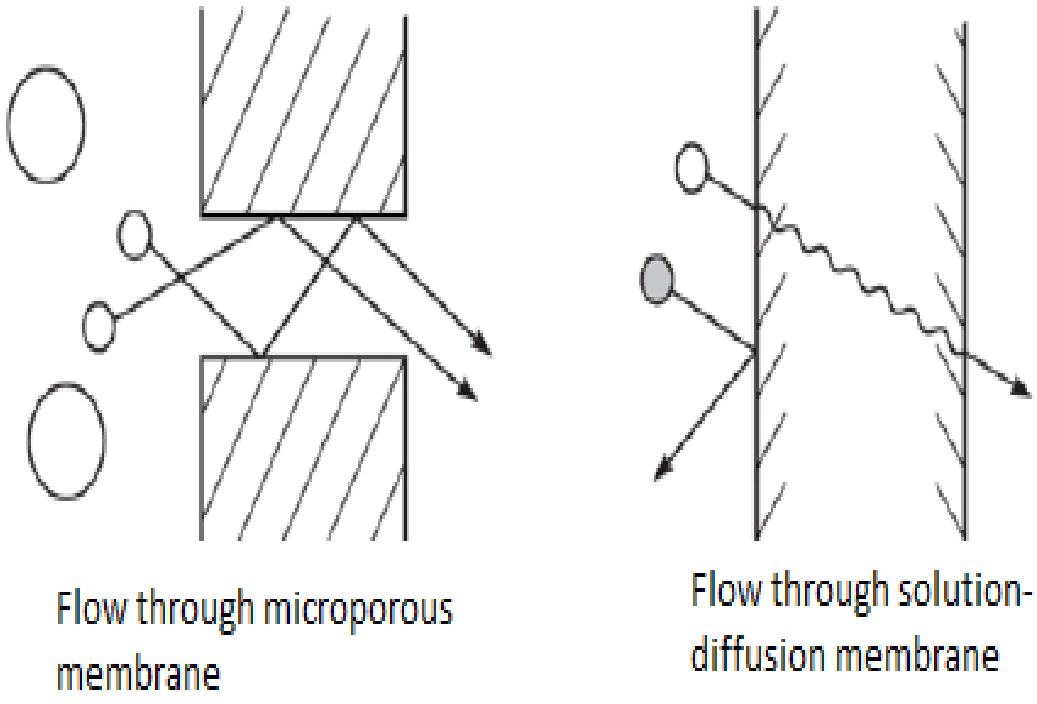

Figure 5: Flows Through the Permanent Pore and Solution-Diffusion Mechanism [24]

According to this model, the concentration gradient across the membrane is only caused due to the chemical pressure gradient because it was examined that pressure across the dense membrane remains constant throughout its highest applied value. The solution diffusion model explaining separation by chemical pressure gradient is given in **figure 6:**

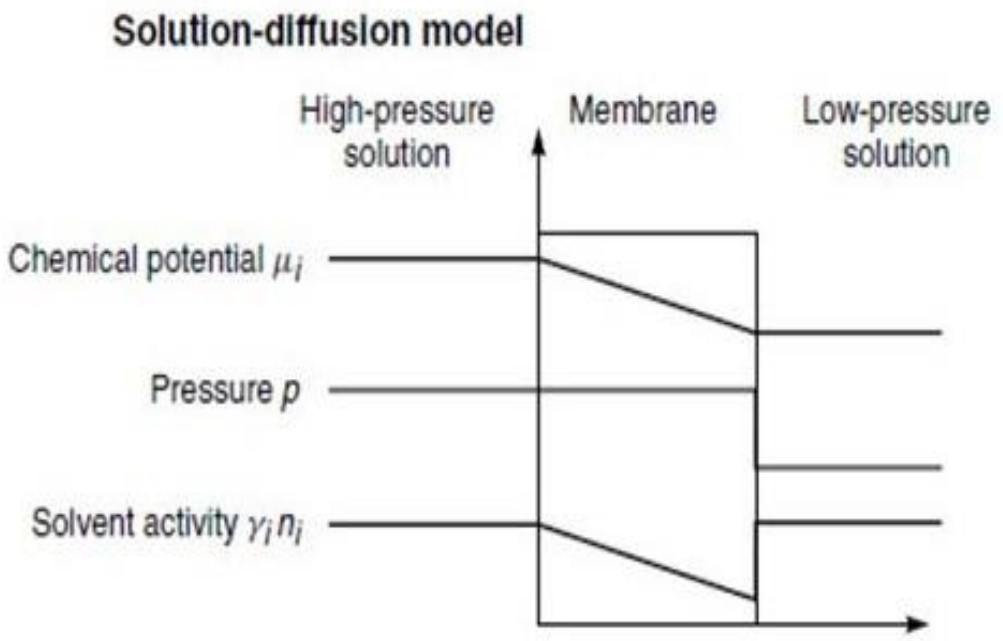

Figure 6: Permeation Driven Through Chemical Pressure Gradient Through The Membrane [24]

1.4.2.2 Pore Flow Model

In this model, the molecules permeate across a membrane by a small pore through a convective flux. It is a totally pressured driven process, in which separation depends on the practical size of the molecules and the size of membrane pore. The pore flow model was defined by Darcy and named as Darcy's law [25].

$$\mathrm{Ji}' = \mathrm{K}'\mathrm{Ci}'\left(\frac{\mathrm{dp}'}{\mathrm{dx}'}\right)$$

Where,

dp'/dx' = Pressure gradient across the membrane interface.

Ci' = Component i concentration in a medium.

K' = Coefficient relates to the medium.

The flux rate for the pore flow model is examined higher than the diffusion flow model because, in the pore flow model, the membrane has a much large, stable and fixed size of pore. The theoretical model for principle membrane separation are given in **figure 7**;

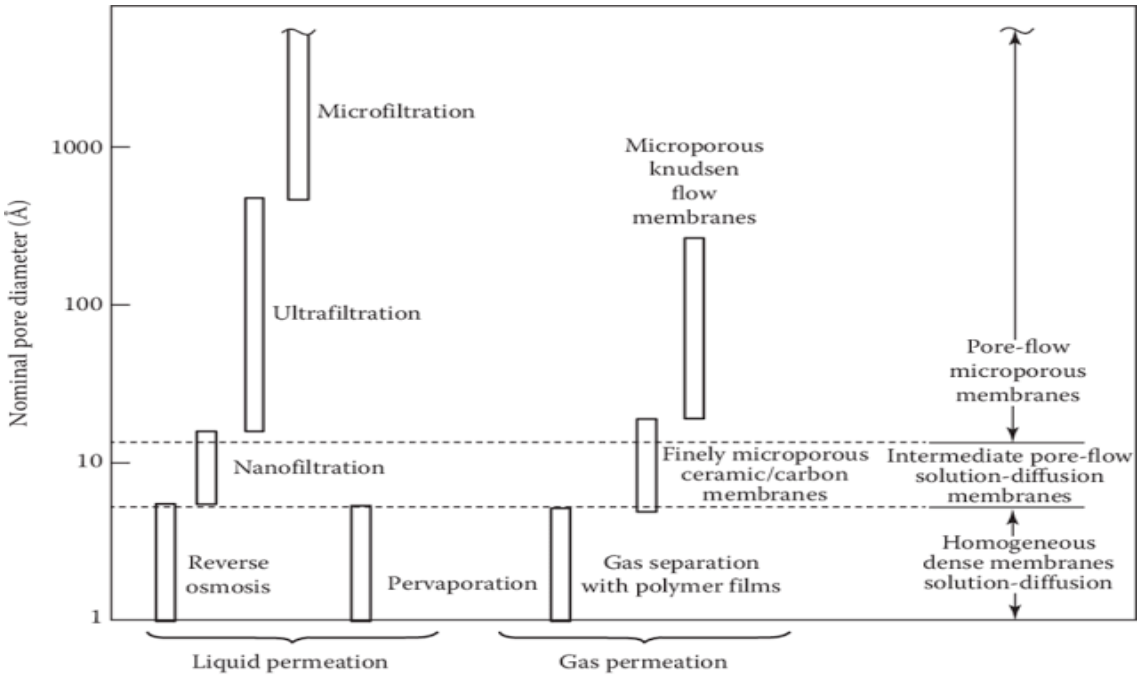

Figure 7: Theoretical Models for the Principle Membrane Separation Process

There are different categories of membranes used for separation of gas like an inorganic membrane, carbon-based membrane, mixed matrix membrane, hybrid membrane, and polymeric membrane.

1.5 Inorganic Membrane

The inorganic materials have the ability to bear high temperatures. So, they are used to the fabricated membrane for high temperature, gas separation purposes [26]. They are three major types of the inorganic membrane:

- Zeolites based membrane
- Sol-gel based microporous membrane
- Palladium based dense membrane

Molecular sieve based on Carbon, zeolite, and silica is used for the syntheses of the inorganic membrane because it has the ability to resist temperature and chemicals. However, there are some issues related to these membranes; high cost, more brittle, difficult to reproduce, less membrane area and permeability and selectivity related issues i.e. increasing one parameter effect another one [26].

1.6 Polymeric Membrane

The issues related to the inorganic membranes are somehow resolved by using polymeric membrane because it has low cost, easy to fabricate, the high surface area for separation, easily converted in a module and can be easily retrofitted in existing technologies.

In an initial time, when membranes were started using for gas separation purposes, pristine polymers preferred for membrane costing, they were first tested on a lab scale, if they show good result then they were being fabricated in modules form for commercial use. The first polymer which was used on a commercial level for gas separation purpose was cellulose acetate in 1980 [27].

1.6.1. Different polymers used for gas separation membrane fabrication

For gas separation membranes fabrication, a lot of polymers have been tested but only a few of them show good results on the industrial level. Polydimethyl siloxane in a rubbery polymer while polyurethane, polysulfone, polyvinyl amine, polyvinyl alcohol, polyimides and polyphenylene oxide in glassy polymer show better result. So the selection of best polymer for the fabrication of gas separation membranes, which gives selectivity of optimum range and high permeability for a specific component in the mixture of gases. overall, we said that polymeric membranes are much more economical then inorganic membrane [28].

1.6.2. Gas separation phenomena across the polymeric membrane

Polymeric membranes are mostly used for the separation of gases. They are separated on the bases of their diffusion rate and their solubility coefficient with the respective polymers. So the permeability can be also defined as "the product of solubility (S) of the respective gas to the diffusivity (D) of that gas in a polymer". Therefore, the solution-diffusion model represents the permeation across the non-porous membranes [29, 30].

The result of the fabrication of glassy polymers for dense membrane shows more selectivity and less permeability for gases like CO_2/CH_4, H_2/CH_4, and O_2/CH_4. In polymeric membranes, the polymeric materials increase the selectivity so that to provide better transport to one component across the membrane as compared to the other mixture of gases.

The solution-diffusion model and Knudsen-diffusion model are most of the time responsible for the gas permeation across the porous as well as dense membranes [29]. The gas separation phenomena across the polymeric membrane is shown in figure 8. In this figure the solution diffusion, molecular sieving and facilitated transport phenomena are shown.

Following steps in which gas flow across the polymeric membrane [29];

- At the upstream side, the gas at high pressure first dissolves in a polymeric material
- In the second step, due to the concentration gradient on both sides of the membrane, the gas diffuses across the polymeric material
- In the third step, at downstream sides, due to low pressure, the gas desorbs

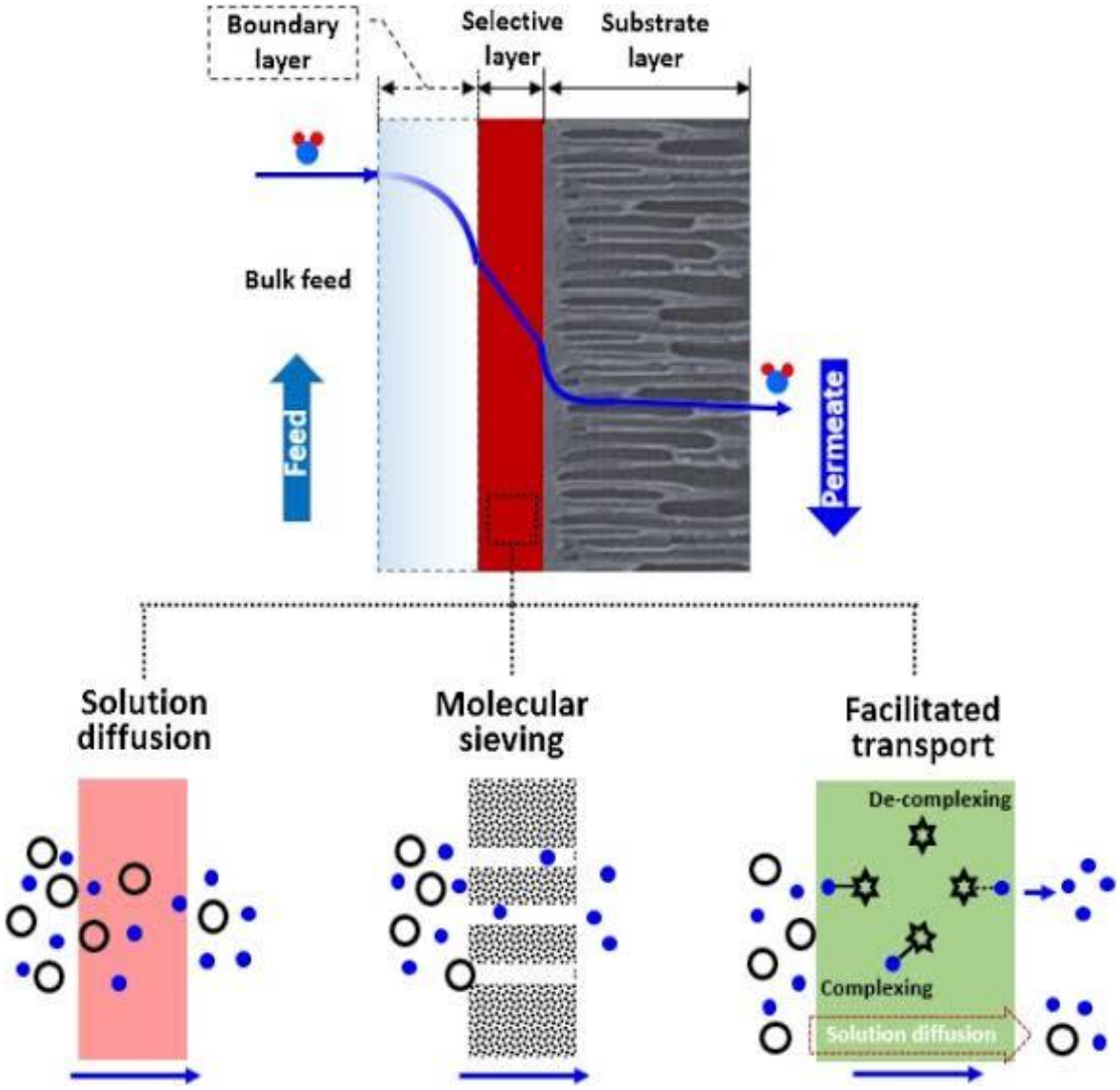

Figure 8: Gas Separation Phenomena Across the Polymeric Membrane [31]

The permeability and selectivity of polymeric membranes are inverse in relation to each other i.e. increasing one of them will lead to a decrease of the other one. **Figure 9** shows the Robinsons trade-off Graph for CO_2/CH_4 Separation.

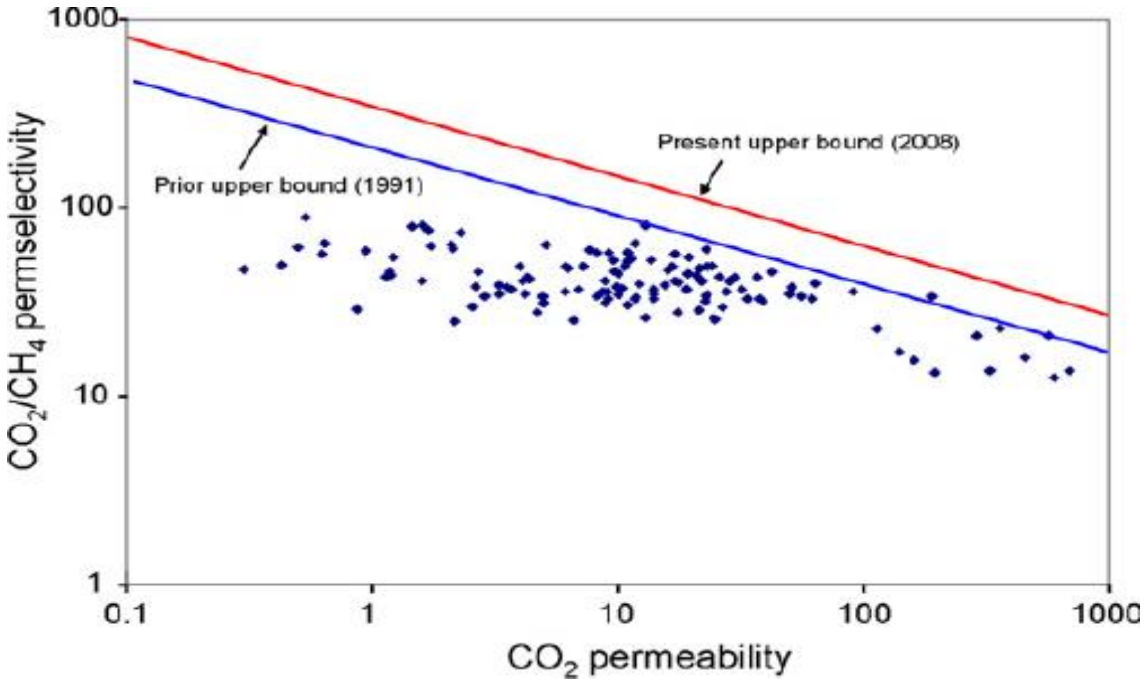

Figure 9: Robinsons Trade-off Graph for CO_2/CH_4 Separation [32]

1.6.2.1. Robinsons Trade-off Graph

Robeson plot the values of permeability and selectivity for small gaseous molecules like CH_4, O_2, CO_2, N_2 in a graph, by permeating these gaseous through different polymeric membranes and set the upper bound limit for the permeability and selectivity called as Robinson trade-off [20].

Because of some issues related to selectivity and permeability in these modules further improvement was needed to increase the result for separation of gas through membrane. So due to high fluxes and high selectivity, facilitated transport membranes (FTM) are became more attractive competent for gas separation.

1.7. Facilitated transport membrane (FTM)

The FTM's are one of the emerging techniques used for the separation of CO_2 from the mixture of gases on the commercial level. In these membranes the carrier agents which are incorporated in it, react reversibly with the desired gas component. So, another transport mechanism is created in membrane, in addition to the simple solution diffusion mechanism. The gas which are required to separate, first dissolved in membrane and

diffuse down a carrier gas complex concentration gradient. The facilitated transport mechanism for CO_2 gas shown in figure 10 [31].

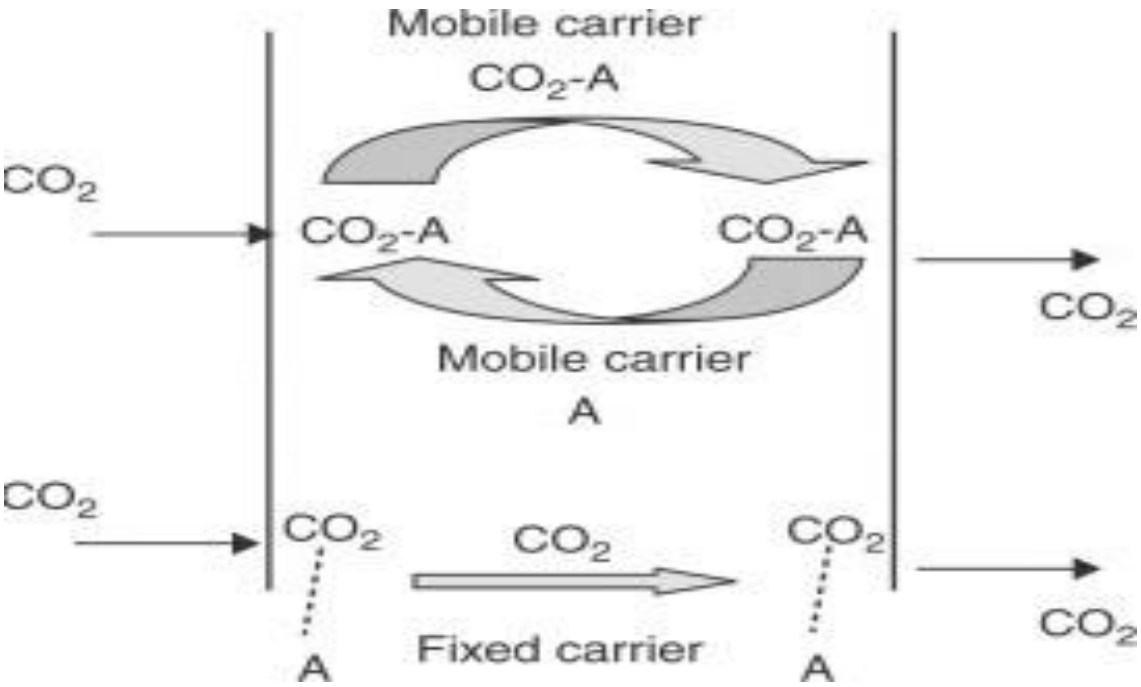

Figure 10: Facilitated Transport Presentation [33]

The carriers make weak bonds with one of the gas feed components reversibly and accelerate their transport across the membrane. Water act as a major carrier in these membranes, so in swollen form, these membranes perform better. While on the other hand, the flux of other gas components is defined by the solution-diffusion mechanism, along with some CO_2 molecules. So to achieve better results of separation for FTM, it is necessary to increase the facilitated transport across the membrane, while decreasing the transport through diffusivity and solubility. The main facilitator is the carrier molecules which provide facilitated transport to species [34].

The general equilibrium equation shows the transport mechanism across the FTM is given be

$$C+P \rightleftharpoons CP$$

$$K = \frac{[CA]}{[C][A]}$$

Where,

C = carrier molecules.

P = the permeating gas component.

CA = permeate and carrier complex.

K = equilibrium constant.

The role of the equilibrium constant is very important because it is used to calculate the concentration of carrier-permeate complex on either side of the membrane. So it is necessary to calculate the optimum value of the equilibrium constant to check the feasibility of FTM. From literature, two assumptions were considered in order to simplify the transport phenomena across the FTM [35]

1. The diffusion rate is considering much slower than the chemical reaction rate across the membrane.
2. The transports through carrier molecules are considered much more than transport through diffusion phenomena.

The amine functional group attach to filler like CNC which also act as a carrier react with CO_2, described by zwitterions mechanism proposed by Caplow [36] and Danckwerts [37]. In this mechanism CO_2 react with amine functional group to form zwitterions as an intermediate.

The better results are obtained in water swollen condition because in swollen condition, hydration reaction with CO_2 would enhanced in presence of amine group. CO_2 transport in form of bicarbonate and carbamate [38].

The carrier gas reaction products diffuse down their concentration gradient to the other carrier agent. The figure 11 shows the FTMs based on amine group;

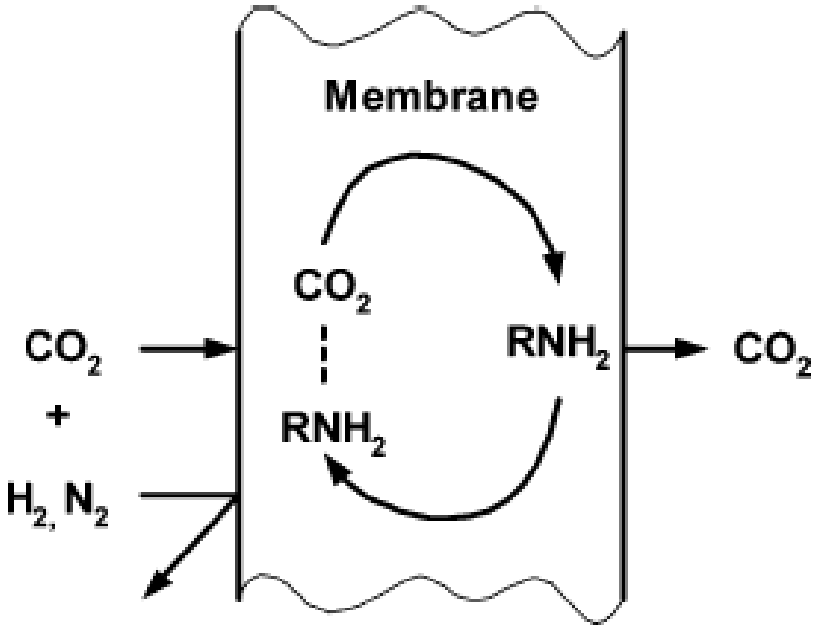

Figure 11: FTMs Mechanism Based on Amine Functional Group [31].

Initially, the liquid supported membrane used as a FTM but these membranes were not suitable to use on a commercial level due to the issue of instability. This instability of liquid support was due to three factors:

1. Membrane liquid evaporation (liquid solvent).
2. Membrane liquid explosion above their bubble point.
3. Carrier agent degradation is due to permeating molecules like water, H_2S.

To resolve this issue, reducing the pressure difference across the membrane was an effective factor. Different methods were used to control the pressure difference:

- Use of sweep gas (convenient at lab scale).
- Use swollen membrane (water or glycerol for swelling purpose).
- Replacement of liquid selective support with permeable, non-selective multilayer polymeric support.

Efforts for many years, researchers were not got success to produce a stabilized liquid membrane model. So, the direction of research was moved toward the solid membranes, to use it as an FTM. The researchers tried to make a membrane, in which the carriers

molecules were covalently bonded with a polymer matrix, but their result was not satisfactory. So, the second approach is to make such FTM in which the polymer by itself acts as a partial solvent for the carrier. This new approach gives better results. There is also some restriction related to these membranes like problems related to the percolation threshold (carriers loading effect on facilitated transport). So, the role of percolation threshold is very important for proper functioning of these membranes. It is that point at which the sites of carrier molecules come close to the complex molecules, so they easily carry these complex molecules from one side of carrier to other sites of carrier. FTM is economical for CO_2 capture due to their better results.

1.7.1 Transport Through Facilitated Transport Membrane (FTM)

The main focus of this study is, how to optimize the performance of FTM. In FTM the moving carriers are embedded within a membrane polymeric matrix. Usually, two mechanisms are occurring for the transport of CO_2 in FTM:

- Solution diffusion mechanism
- Carrier-mediated mechanism

The irreversible reaction of CO_2 with carriers' molecules and then selective permeation of CO_2 through the membrane. While N_2 and CH_4 which are inert and non-reactive gases follow the mechanism of solution diffusion for exclusive permeation [39]. Fick's law of diffusion defined the Mass flux "J", which described the permeation of component "A" of gas through the membrane, [35].

$$J' = -D'\left(\frac{dc'}{dx'}\right)$$

Where,

J'= mass flux.

D'= diffusion coefficient.

Dc'/dx' = driving force (concentration gradient)

For liquid-gas interface, Mass flux can be modified;

$$J_A = \frac{D_A}{L}(C_{A,0} - C_{A,L})$$

Where,

L = Thickness of the membrane.

However, if we conceded the facilitated transport across the membrane with carrier molecules, above equation becomes more complex. Because the carriers also make their contribution in transport of desired component of feed gas across membrane. Therefore, sum of Fick and carrier-mediated diffusion will be the total mass flux;

$$J_{A=}\frac{D_A}{L}(C_{A,O} - C_{A,L}) + \frac{D_{A,C}}{L}(C_{AC,O} - C_{AC,L})$$

Where the first term is for Fick diffusion and the second term is for carrier-mediated diffusion. The carrier-mediated phenomena were explained in the literature [40]. So, from above equation 6 it is clear that if we want to improve the carrier-mediated transport, we have to reduce the thickness of the membrane. Secondly, we have to improve the selective nature of carriers for the desired component.

For this purpose, research is focused on such polymers, carriers that can further improve the desired permeation result and resolve the issues related to the above parameters. Different types of particles used as filler which provide fixed cite carriers and facilitate transport to the desired component of gas to permeate across the membrane. In these carriers, some are inorganic like CNTs, MOFs, and various zeolites. The new generation of membranes is fabricated by adding these inorganic particles in a polymer matrix for gas separation. By adding these particles, the permeation properties are much improved [41-43]. Due to some issues related to these inorganic particles, new ideas of fabricating an FTM's, in which the carriers' particles used were bio fibers. Bio fibers available in trees are a major source of cellulose. The reason for adding bio fiber is, it is natural, biodegradable, their swelling properties in the presence of moisture [44] and their compatibility with water-swollen polymers [45]. Due to these properties, the attention of researchers diverted toward cellulose.

1.8 Polymer and filler selection for FTMs casting

1.8.1 Cellulose as a filler

In the ecosystem, cellulose is the most abundant available polymer. It is natural, renewable and biodegradable. It has a Nano-sized microfibril chain arrangement, in which both amorphous and crystalline parts are present. It is mostly present in the cell wall of plant cell, highest content of cellulose is found in cotton, are approximately 90% [46].

1.8.2. Structure of Cellulose

Cellulose is homo-polysaccharides, having monomers of glucose linked to each other by β-1, 4- glycosidic bonds. Figure 8 given below shows the structure of cellulose. It is highly stiff and hydrogen bonding in chains give him structural strength. it has a hydrophilic nature due to hydroxyl groups, low density, length to diameter ratio is high, large surface area, and good mechanical strength. More ever, abundant hydroxyl groups in cellulose structure provide the option of surface modification like functionalization, esterification, sialylation and polymer grafting [47]. These all properties attract the researcher toward cellulose.

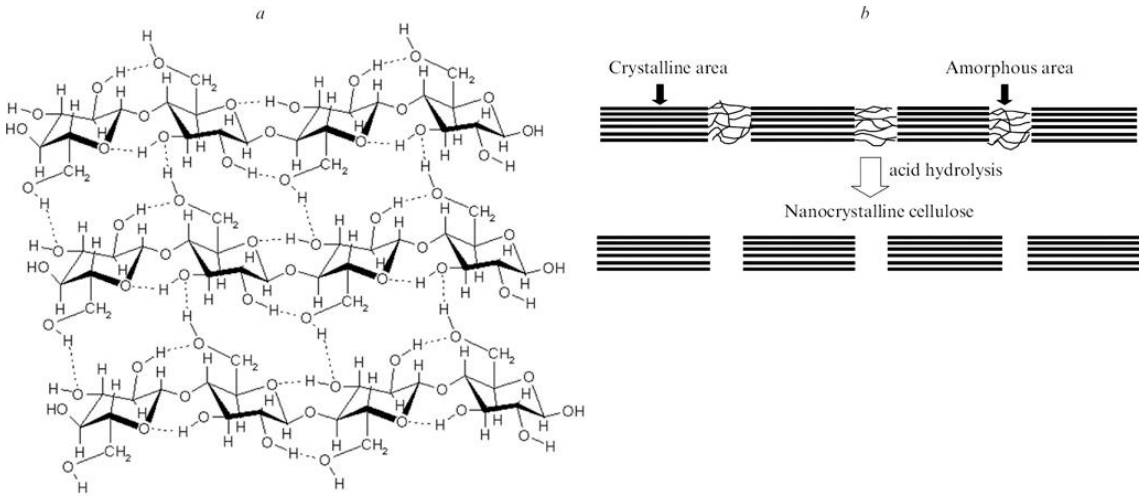

Figure 12: Structure of Cellulose [48]

1.8.3. Nano Cellulose

Nano cellulose is Nanoparticles, obtained from cellulose. These particles have must one dimension less than 100 nm, to conceder as Nanoparticle. Nano cellulose have two types;

- Cellulose Nanofibers (CNF)
- Cellulose Nanocrystal (CNC)

1.9.1 Cellulose Nanofibers (CNF)

Cellulose Nanofibers (CNF) are also called micro fibrillated cellulose. It has a dimensional ratio of 5-20 nm. CNFs are pseudoplastic and have a highly viscous nature while on dispersions. By increasing its concentration above than 1%, it shows a gel-like behavior. This can make problems in some applications. It might be used as a barrier because it can form strong, dense and impermeable inter fibril bond. So, it might be used as a barrier.it can also use in an ultra-absorbent aero gels formation because of its low weight and high strength [49].

1.9.2 Cellulose Nanocrystal (CNC)

Cellulose Nanocrystal (CNC) particles have stiff, rode like structure. It has a width of 2-30 nm with several hundred nm of length. We can prepare it from acidic hydrolysis of cellulose i.e. hydrolysis of hardwood, micro cellulose, wheat straw algae, sugar beet, and cotton, etc. [46].

1.10 Cellulose Nanocrystal (CNC) Preparation

Cellulose Nanocrystal (CNC) can be prepared through different methods. Two of which are discussed below;

1.10.1 Preparation from Micro Cellulose

The Nano cellulose crystals are obtained from micro cellulose. The micro cellulose was added in deionized water and then stirred for 24hr. After stirring, the suspension was sonicated for 2hr. To maintain the temperature normal, the beaker was placed in an ice bath during sonication. The turbidity appeared which indicates the CNC's formation. The supernatant was discharged into other vessel and then by using vacuum filtration the water was removed and dry CNC was obtained [50].

1.10.2 Preparation from Acidic Hydrolysis

Initially, cellulose-containing pulps are treated in strong acid like sulphuric acid due to which pulp is degraded. In this process, first of all, the uppermost exposed fibers are degraded then followed by reducing end groups and crustal surface. Following parameters should be fully controlled during hydrolysis;

- Reaction time
- Reaction temperature
- Acid concentration

The sulfate group of sulphuric acid replaces the hydroxyl groups of cellulose in a crystalline region. If the time of reaction will shorter, the high degree of polymerization is obtained, while if the time of reaction will longer, the cellulose crystal will completely hydrolyze [46]. More ever, reaction temperature, acid to pulp ratio also plays a role in cellulose hydrolysis. Temperature variation observed from the range of 25 to 65^{o}C from 15 minutes to 18hours [46]. After hydrolysis, dialysis was done for purification and small rods like crystal of cellulose were obtained. CNCs were in suspension form [51, 52].

1.11 Characteristics and Applications of Cellulose Nanocrystal (CNCs)

CNCs have the following unique characteristics like its high mechanical strength, low weight, and high swelling character. The mechanical strength of CNCs has a range of 7.5-7.7 GPa, which is very high then Kevlar and steel wire. Their elastic modulus was around 140 GPa [53]. The mechanical properties were calculated through the following tests; AFM, inelastic X-ray, Raman scattering and XRD analysis. Moreover, swelling character was studied in humid environments, its moisture uptake properties were much better, the resistance in mechanical stretching of CNCs structure is due to strong hydrogen bonding [44]. The characteristic of CNCs which are discussed above gives them more importance on industrial level. Some of their applications are following.

- CNCs are used in paper industries for enhancing the strength of papers.
- CNCs are used in biocomposites as a filler for enhancing their mechanical properties.
- CNCs are used in food industries for food stabilizing.

- CNCs are used in films, paints, and automotive industries.
- CNCs have good absorbing properties so, used in tissue paper production[46].

These unique properties of CNCs which are discussed above, make it compatible with water-swollen membranes. Cellulose and their derivatives are also used in microfiltration, ultrafiltration and dialysis membranes. Mostly CNCs were used as a filler in membrane technologies for CO_2 separation from a gas mixture [45]. Their hydroxyl groups provide facilitated transport to the CO_2 across the membrane. Following are the pathway of reversible reaction for CO_2 transport;

$$\mathbf{CO_2 + OH^- \leftrightharpoons HCO_3^-}$$

At permeate side HCO_{3-} split down into CO_2 and OH-, while CO_2 released from the membrane. The research was done on CNCs/PVA membrane and their permeability, selectivity, mechanical, thermal and swelling properties were investigated [54].

1.11.1 Amination of Cellulose Nanocrystal

The focus of this work is on biogas upgrading by removing CO_2 from it. So, it was observed from the different researches, that amine scrubber used for CO_2 removal, have very better efficiency on the industrial level as compared to others [55]. Similarly, CNCs as filler used in FTMs for CO_2 removal, which also shows better results of permeability and selectivity [56]. While on the other hand, CNCs structure has a hydroxyl group on his reducing end which can be replaced by another functional group. Amine modified aerogel of CNCs was also used for CO_2 capture through covalent bonding [57]. Therefore, in this work, the hydroxyl group of CNCs is replaced by Amine functional group. and then used as filler in PVA polymer matrix and membrane are cast and their properties like permeability and selectivity are studied.

1.12 Selection of Polymer for Membrane Casting

As discussed above, this work is focused on biogas upgrading by CO_2 removal for the gas mixture. While PVA is selected as the main polymer Matrix for membrane casting. PVA has good water-soluble properties and polyvinyl acetate hydrolysis gives us PVA. PVA based membrane has high thermal stability, has good barrier properties for oxygen,

feasible than other polymer and environment-friendly nature[58]. Figure 13 shows the molecular structure of PVA;

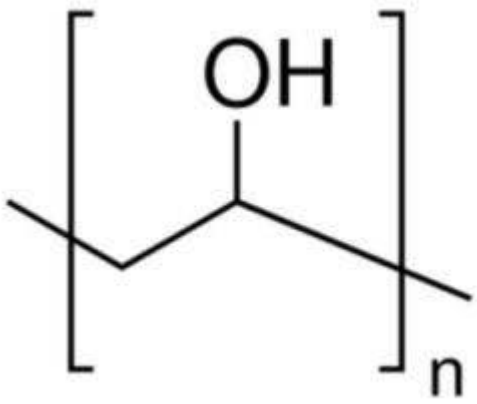

Figure 13: Molecular Structure of PVA

While, the results of PVA and CNCs based FTMs membrane for CO_2 removal, show better results [56]. PVA was also used in a blend with other polymers [59-61] and with different fillers for CO_2 capture[62-64] and show better results. The focus of this work is to fabricate a FTMs based on PVA and aminated CNCs and study their permeability and selectivity results for CO_2 capture from biogas.

1.13 Selection of Porous Support for Dense Membrane Layer Casting

For FTMs, the porous support is needed. So, to cast a dense layer on it. This support provides a mechanical strength against high pressure and also provides thermal stability to the dense layer. There are a lot of porous polymeric supports used for composite membrane costing for gas separation purposes like polyethersulfone (PES), polyvinylidene difluoride (PVDF) and polysulfone (PSF). In this work, polysulfone is used as support for PVA based composite membrane casting. **Figure 14** shows the PSf structure with repeat units;

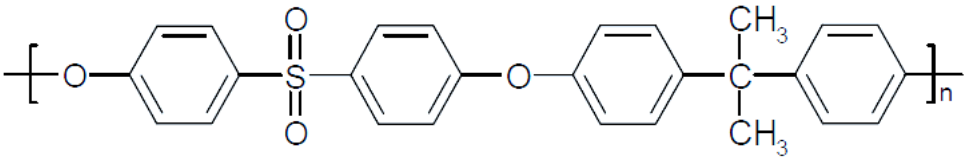

Figure 14: Structure of PSf with Repeating Units

There are following properties of PSF polymer due to which it is selected as porous support for membrane;

- PSF is amorphous, transparent and belongs to the thermoplastic family.
- It has high thermal, hydrolytic and oxidative stability.
- It can be extruded, molded and thermoformed in different shapes.
- It has high strength, high oxidation resistance and good flame retardancy [65].

1.15 Objectives of this Research Work

The efficiency of FTMs based on Am-CNCs filler and PVA as polymer matrix-supported on polysulfone support shows better results for CO_2 removal from biogas, while amine-based scrubber which is used on an industrial level for CO_2 removal also shows efficient results. Similarly, Amine modified aerogel of CNCs was also used for CO_2 capture through covalent bonding. So, the work done in this research is on FTMs, based on aminated CNCs and PVA and the major objectives of this work are following;

- Amination of CNCs
- Characterization of aminated CNCs through XRD and FTIR
- Fabrication of membrane having aminated CNCs as a filler and PVA polymer matrix on PSF support
- Membrane characterization through XRD, SEM, and FTIR
- Permeation testing of membrane i.e. its permeability for CO_2 and CO_2/CH_4 selectivity for biogas
- Optimization of membrane performance parameter for achieving better results.

In the end, results compared with the literature published results. This comparison helps in future work for the optimization and development of FTMs for gas separation.

1.16. Basic outline related to this thesis

In **chapter 1st** detailed discussion on the background related to the different energy resources, its availability, demand, usage, and related issues. Biogas production, its upgrading techniques and usage in the world are discussed. Polymeric and inorganic membranes for gas separation are discussed. Different models used in membrane separation technique are discussed. FTMs are also discussed in detailed. CNCs filler is discussed in detailed. Polymer Matrix and porous support selection are also discussed in this chapter.

In **chapter 2nd** the previous research work was summarized which is related to CO2/CH4 separation, FSC and FTMs development with their separation efficiency. Comparison b/w different polymers and fillers which are added a carrier in membranes for increasing efficiency was also discussed. Most of literature was related to water swollen polymers like PVA and PVAm. Filler like CNCs used as a filler, their amination and water-swollen membranes based on PVA and CNCs are summarized.

In **chapter 3rd** experimental work related to the amination of CNCs, solution preparation, and membrane fabrication was discussed in detailed. The different characterizing techniques used to check the membrane and CNCs characterization like membrane morphology, crystallinity of Am-CNC and membranes and moisture uptake behavior are discussed.

In **chapter 4th** results related to different characterizations and performance of fabricated membranes are summarized and discussed in detailed to understand the work performed. In this chapter research work is also concluded along with future recommendations.

Chapter 2

Literature Review

Globally, the consumption of energy increased nearly twice in 2018 as compared to the average rate of growth in 2010. To fulfill the world energy requirement, fossil fuels are nonrenewable resources, so they will be depleted. The approximate depletion times for coal, gas, and oil are 108, 39 and 36 years respectively. So, world is moving toward sustainable energy resources. Sustainable energy resources are defined as the resources which are equality available for all peoples and also preserve on earth for future generation. Renewable sources of energy withstand themselves naturally without depleting on earth. The contribution of renewable energy resources in world energy demand will be approximately 48% up to 2040. Biogas is one of modern renewable energy produced by Anaerobic digestion, a series of biological processes, in which micro-organisms digest the organic waste material in sealed containers to produce biogas, which has mixture of CH_4, CO_2, and other gases. To increase the energy intensity of biogas, must need to remove carbon dioxide since to improve methane concentration. Therefore, membrane technology (cost-effective, easy to operate and environment-friendly) is one of competitive options for biogas upgrading for CO_2/CH_4 separation. Some of membranes used by researcher for biogas upgrading are; facilitated transport membrane (FTMs), Mixed Matrix membranes (MMMs), fixed-site carrier membranes (FSCs) and Nanocomposite membranes.

2.1. Cellulose Nanocrystals (CNCs)

2.1.1. Cellulose Nanocrystals Preparation

CNCs are one of the most emerging bio fiber materials, have been used in different industrial applications like food, pulp and paper, medicine, cosmetics and as additive. The first time CNCs was prepared by Nickerson and Haberle et al 1947. through acid hydrolysis process using strong H_2SO_4 and HCL. It was found from the test results that in the hydrolysis of glucose, the first reaction was done with the intercrystalline chains of glucose. So, due to which decrease in viscosity was noted while due to moisture effect, the glucose accumulation was noted. The fibers were converted to hydro cellulose crystal

powders. The length of crystals was calculated from range of 280 glucose units for cotton and 110 for viscose rayon. While it was also noticed that HCl was more active compared to H_2SO_4 [66]. Similarly, Dong et al prepared CNCs from powder of filter paper by using a hydrolysis process with 64 wt.% H_2SO_4 at 45^oC for 1hr. CNCs obtained from the hydrolysis was 70 to 170nm in length and 7 nm in width [67].

2.1.2. Properties of Cellulose Nanocrystals (CNCs)

Ping Lu et al. discuss the crystallinity of CNCs which was reported from a range of 65% to 95% in literature, depends upon its source of extraction. The CNC's bending strength and modulus were estimated and measured by Sturcova et al. which had very impressive results range from ~10 and ~150 GPa, respectively. CNCs have much more strength than steel. Due to its high modulus value 65 j/g compared to steel have 25 j/g, CNCs can be used in Nanocomposite as a reinforcement additive [68].

Mi-Jung Cho studied the tensile modulus of CNCs with PVA composites. According to which, as the concentration of CNCs was increased up to 5wt.%, the tensile strength was increasing but after 5wt.% its strength was decreased due to agglomeration of CNCs in polymer Matrix [69].

Some of the mechanical properties of CNCs with PVA Nanocomposite membrane were investigated by Z. Jahan et al. the elastic modulus of CNCs based PVA membrane was reported, in which at relative humidity of 0 and 53%, by increasing CNCs concentration above 1.5wt.%, elastic modulus decreased. While at 93% RH the result was higher than 0 and 53% RH at same concentration. By increasing concentration above 1.5 wt.%, results of 93% much less than other two. Tensile strength pattern was opposite to the elastic modulus i.e. increasing concentration of CNCs increased the strength while decreasing RH increased the tensile strength. The tensile strength calculated was 132 and 155 MPa for 53 and 0% RH. Similarly, increasing concentration also increased the crystallinity index of composite membrane strength.

The swelling properties of CNCs based PVA composite membranes were also investigated at 0%, 53% and 93% RH. According to results, the moisture uptake of Nanocomposite membranes was increased up to 1.5wt.% CNCs concentration but further

increase in concentration caused to decrease moisture uptake. While the permeation results of 1.5wt.% CNCs concentered was reported high then other[70].

2.1.3. Amination of Cellulose Nano Crystal (CNCs)

K. Singh et al successfully functionalized the CNCs by Amine functional group and then used it for the purpose of water purification by removing Cr(III) and (VI). The result shows that there was a significant development in the removal of Cr(III) and (VI) up to 94.84% and 98.33% respectfully [71].

L. Jin et al used amino-functionalized CNCs as anionic dyes adsorbent.it was noted from the results that amino-functionalized CNCs show high adsorption capacity for anionic dyes in a solution. While its better result was noted in an acidic medium [72].

X. Wang et al functionalized spherical Nano cellulose aerogels with an amine group and characterized it with different techniques like XRD, FTIR, NMR, TGA, and SEM. It was studied that when the aerogel was dried by supercritical CO_2. it gives Nanoporous structure having large surface area up to 262 m^2/g. while freeze-drying gives honeycomb-like structure having polygons and circles. Its surface area was up to 120.4 m2/g. it was noted that Amino based CNCs aerogel could have also the potential for CO2 capture through covalent bonding.

2.2. Fixed Sites Carrier Membranes

A fixed site carrier membrane is an emerging technique used for gas and liquid separation. It has the ability to improve permeability and selectivity results. Some of the mathematical models for describing mass transfer across the FTMs with fixed site carriers were also developed.

The fixed-site-carrier membrane fabricated from polyvinyl amine (PVAm) in NTNU, show impressive results of high selectivity for CO_2/CH_4, CO_2/N_2, CO_2/H_2 and high permeability for CO_2 [61, 73, 74].

Fixed site carrier (FSC) membranes are in solid form or maybe carriers bound to the polymer matrix. The polymer matrix of solid membranes has carriers in dissolved form or in dispersed form, so the carrier which has reactive nature is immobile, the permeating components are transferred from immobile carrier site toward carrier site.

After a lot of research, the researcher got success to make a covalent linking of amine-containing functional groups to the matrix polymer [35]. These FSC membranes are now operating at piolet scale, their permeation properties show stability under continuous testing in real operating conditions with impurities present [74, 75].

Baker mentions the studies of Sandru et al [76]. and Deng et al.[39]. According to which fixed-site carriers polymeric membranes may be first FTM which was used on industries level [35].

Some other FTMs like blend of PVAm/PVA coated as a dense, selective layer on PSF (polysulphone) support [77], composite membrane of PVP/PSF (polyvinylpyrrolidone) [78], membrane has both mobile carriers (2-aminoisobutyric acid, AIBA-K, and $KHCO_3$-$K2CO_3$) and fixed site carriers (PVAm) blend in PVA [79].

J.M. Hong et al discussed the mathematical model, (2. Series RC circuit model) to analyze the FSCs polymeric membranes. The extended the existing single RC circuit model, which was designed on concentration fluctuation, electron transport analogy in a parallel resistor-capacitor and mass transfer across FTMs. The work done in this research was based on a series of parallel RC circuits for studding four diffusion pathways and demonstrated the transfer of solute between carrier and matrix. When the model was compared with experimental data for O2 transport for different polymers it gives much better results as compared to the single circuit model [80].

S. Rafiq et al discussed the CO_2 capturing efficiency through Facilitated Transport Membranes and Composite Membranes in detailed. His discussion was the focus on development of FTMs based FSCs and effect of silica Nanoparticle in polymeric membrane for CO_2 capture. Complexing agents work as a carrier in FTMs which reversibility react with desired component (like CO_2) of feed. Other non-reactive components like CH_4, N_2 across the membrane through Fickian diffusion.CO_2 move across the membrane in form of carbamate and carbonate in the presence of water in humidified feed gas [81].

H. Matsuyama et al studied different aminated polymers for FTMs were used to CO_2 capture and it was studied that, at water-swollen conditions, these membranes give better results than dry form [82].

Kim et al also studied the effect of water humidification of feed on CO_2 removal for PVAm based FTMs. The increased result of permeability and selectivity was noticed in water humid condition. The CO_2 transport mechanism was also discussed by Kim. Results for PVAm based FTMs coated on PSF sheet shown ideal selectivity of greater than 1000 for CO_2/CH_4 [73].

W. Ho et al discussed the FSCs membranes, in which the carrier may be mobile or fixed to the polymer chain or carrier attached to functionalized Nanoparticles. W. Ho fabricated first time sulfonated polybenzimidazole copolymers (same properties like PVA) for mixed matrix membranes. In this copolymer blend of Poly ethylenimine and poly (allylamine) (PAA) was used as a carrier.

The effect of moisture, temperature and membrane composition was studied. The effect of water on membrane performance was positive while the best optimal temperature was up to 100^oC was examined. The highest permeability examined for CO_2 was 2539 barriers with the selectivity of 64.9 [83].

Zang et al worked-on amine-based polymer (like polyvinylamine (PVAm), (N-vinyl-g-sodium aminobutyratecoco-sodium acrylate) and pentaerythrityl tetramethylene diamine) for fabricating FSC membranes. The resulting membranes showed good results for CO_2 permeance across the membrane.

These membranes were tested for pure single gases (CO_2 and CH_4) and for mixed gases (CO2/CH4) of 50wt.% of each. The results for pure gases at 26^oC and 0.013 atm CO_2 pressure, the dense membrane on PSf support give permeance of 7.93×10^{-4} cm^3 /cm^2 s mmHg for CO_2 while selectivity of 212.1 for CO_2/CH_4. The results for mixed gas testing at 26^oC and 0.016 atm CO_2 pressure for CO_2 permeance was 1.69×10^{-4} cm^3 /cm^2 s cmHg and selectivity of 48 [77].

Matsuyama et al fabricated an FSC membrane based on a blend of polyethyleneimine/poly (vinyl alcohol) (PEI/PVA) for CO_2 permeance. The PEI polymer was in an entanglement with PVA polymer chain. The study showed that increasing the partial pressure of CO_2 in feed caused decreased CO_2 permeance while shown no effect on N_2 permeance. So, it concluded that only CO_2 was transported through fixed carriers. It was also noted that increasing the wt.% of PEI in blend dramatically increases the CO_2

permeance. These membranes showed selectivity results for CO_2/N_2 gas of 160 and after heat treatment reached 230 at CO_2 partial pressure of 0.065 atm [84].

L. Deng et al worked on dense membranes of PVA/ PVAm blend cast on PSf support for CO_2 removal. The membranes were first humidified by water moisture to its maximum uptake capacity before permeation testing. The gas mixture of CO_2/CH_4 (10% of CO2 by volume) was tested and results were calculated through gas chromatography.

The highest permeance reported for CO_2 at 2 bar pressure, 25°C temperature and at 90% humidity was 0.3 m^3 (STP)/m^2.bar.hr. and selectivity of 35. The PVAm addition in PVA increased the permeation results for CO2/CH4 gas [85].

L. Deng et al also worked on FSC membranes based on PVAm/PVA blend with carbon nanotube as filler. The results show that CO_2/CH_4 selectivity for low-pressure range i.e. 2 bar to 5 bar was 45 while the permeance of CO_2 was reported up to 0.35 m^3 (STP)/m^2 h bar. The filler (CNTs) concentration up to 1.0 wt.% gives good results of durability against compaction at high pressure [86].

M. Saeed et al worked on FTMs based on water-swollen PVA membrane with carbon nanotubes as a filler. The PH of membrane costing solution was adjusted to basic and membranes were examined for post-combustion CO_2 removal at the humid condition with law CO_2 partial pressure. The concentration of filler was used from range of 0 to 2% (w.r.t PVA) and PH was adjusted from 5 to 12.

It was noted that the CO_2 permeance was increased from range of 0.18 m^3(STP)/m^2bar h to 0.44 m^3(STP)/m^2bar h with constant selectivity of 60, with increasing filler concentration and PH while the degree of swelling of the membrane was also increased from 154 to 254. The thickness was decreased with increasing filler concentration and PH which further increase the permeance up to 0.48 m^3(STP)/m^2bar h [87].

M. Saeed et al also worked on water-swollen PVA nanocomposite membrane with two fillers like carbon Nanotube and mimic enzyme for CO_2 removal. A thin dense membrane of PVA was fabricated and has mimic enzyme and CNTs on support through the dip-coating technique. It was examined that the thickness of the membrane was directly affecting polymer and filler concertation.

The optimal result was reported for mimic enzyme at concentration of 0.005mmol/g. the results for CO_2/N_2 separation were also studied at different concentrations of CNTs range

from (0, 0.5, 1.0, 1.5%) and different pH like 5, 9 and 12. The CNT's addition improved the swelling properties of membranes. The highest result reported for CO_2 permeance at 1.0 wt.% CNTs and 12 pH was 0.98 m^3 (STP)/m^2 h bar and selectivity of 120 which was 30% higher for CO_2 permeance and 15% higher for CO_2/N_2 selectivity compared to membrane without CNTs filler [88].

J. Torstensen et al worked-on CO_2 removal from flue gas using PVA nanocomposite membrane with different size CNCs as a filler. In this research work, the CNTs were replaced by CNCs which shown improvement in permeation results. The results reported for CO_2 permeance was 127.8 GPU selectivity was 39 for CO_2/N_2. It was also studied that smaller the size of CNCs with high charge will improve the permeation results [89].

Z. Jahan et al worked on PVA nanocomposite membranes with CNCs as a filler for separation of CH_2/CH_4 at high pressure. The following results was concluded in this research work; when CNC was added in a membrane fabricating solution, it increased the swelling properties of membrane, increased the thickness of the dense layer, increased the crystallinity of membranes. The best result for permeance and selectivity of CO_2 were reported on 1 wt.% CNCs concentration and at higher pH value.

It was also studied that the permeance results have inverse relation with increasing feed pressure. The best results reported for CO_2 permeance are 0.29 m^3(STP)/(m^2-h-bar) and selectivity of 43 for CO_2/CH_4 separation [56].

Z. Jahan et al also worked on PVA nanocomposite membranes having phosphorus functionalized CNFs as filler for biogas upgrading under high pressure. The PVA membranes were fabricated with different concentrations of PCNFs range from (0, 0.5. 1.0, 1.5, 2wt.%). The thickness was increased with increasing PCNTs concentration. The best result was reported on 1 wt.% PCNTs concentration at 12 pH. The maximum permeance reported for CO_2 was .21 m^3(STP)/(m^2-h-bar) with the selectivity of 46 for CO_2/CH_4. It was also reported that increase in feed pressure inversely affects the permeance of CO_2 [90].

Table-3: Summary of PVA Membranes with its Blend and Filler

Polymer	Filler	Pressure/ Temp	Permeance	Selectivity	Ref.
N-vinyl-g-sodium aminobutyratecoco-sodium acrylate and pentaerythrityl tetramethylenediamine	Nil	0.013atm/ 26^{o}C	1.69×10^{-4} cm^3. cm /cm^2. s. cmHg	48	[77]
(PEI/PVA)	Nil	0.065atm/ 25^{o}C	$8.5\times10^{-8}cm^3$ cm/cm^2. s. cm Hg	160	[84].
PVA/PVAm	Nil	2 bar/ 25^{o}C	0.3m^3(STP)/ m^2.bar.hr	35	[85]
sulfonated polybenzimidazole copolymers	Polyethyleneimine/ poly allylamine (PAA)	30psi/ 100^{o}C	2539	64.9	[83]
PVAm/PVA	carbon nanotube	2 bar/ 25^{o}C	0.35 m^3 (STP)/ m^2 h bar	45	[86]
PVA	carbon nanotubes	1 to 3 bar/25^{o}C	0.44m^3(STP)/ m^2bar h	60	[87]
PVA	carbon Nano tube/ mimic enzyme	1 to 3 bar/25^{o}C	0.98 m^3 (STP)/ m^2 h bar	120	[88]
PVA (for flue gas)	CNCs (different size)	1 bar /25^{o}C	127.8 GPU	39	[89]

PVA (for biogas)	CNCs	5 to 15 bar/25^{o}C	0.29 m^3(STP)/ (m^2-h-bar)	43	[56]
PVA (for biogas)	PCNFs	5 to 15 bar/25^{o}C	.21 m^3(STP)/ (m^2-h-bar)	46	[90]

Chapter 3

Experimental Work

3.1. Materials Used

Commercial grade, flat sheet, ultrafiltration membrane, based on polysulfone (PSF) with the molecular cut-off weight of (50,000) was purchased from Alfa Laval. CNCs with average width of 12nm and average length of 170nm were purchased from cellulose lab. Polyvinyl alcohol (PVA) with molecular weight of (89,000-90,000) and 98% hydrolyzed was purchased from Sigma Aldrich. Potassium peroxidisulphate, ethylene diamine, acrylamide and deionized water used as the main solvent, was also purchased from Sigma Aldrich.

3.2. Amination of Cellulose Nanocrystal (CNCs)

For CNCs amination a standard practice [71] has been followed. First of all, deionized water was taken in a beaker and then suspension based on 2 wt.% with CNCs, was prepared. Then potassium Peroxydisulphate 1 wt.% (with respect to CNCs) was added as an initiator in a CNCs suspension. The solution was kept for 10 min stirring. After this, acrylamide of 1wt % (with respect to CNCs) was added in suspension and kept for 90 min stirring at 50^{o}C.

With the help of vacuum filter, the initiated CNCs were separated from the solution and washed with deionized water. Then, equal volume to distilled water, ethylene diamine was added to initiated CNCs and reflux for 8hr. after completion of reflux aminated CNCs were prepared, which was separated and dried with help of vacuum filter process. XRD and FTIR characterization of aminated CNCs was done, for the conformation of amine functional group attachment.

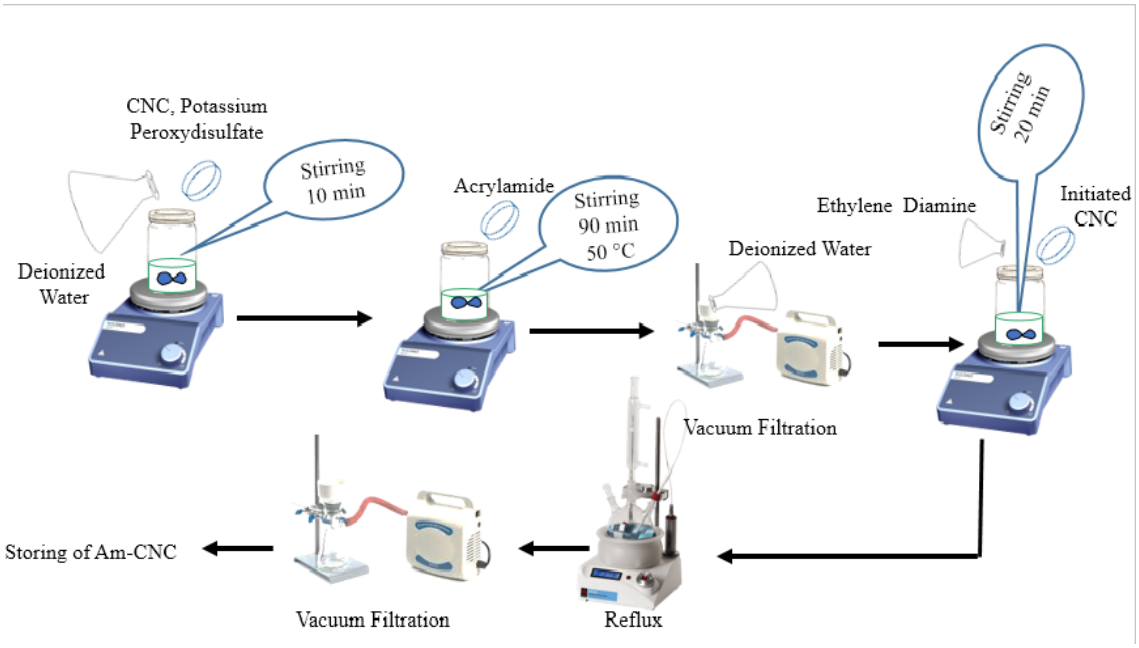

Figure 15: flow Diagram of Amination of Cellulose nano Crystal

3.3. Making of Solution

PVA mixture of 2 wt.% was prepared by adding it in deionized water. Then the mixture was kept for stirring at 700 rpm, at 90^{o}C for 3hr and left the solution for overnight rolling on the mechanical roller, to obtain a clear solution of PVA.

Aminated-CNC with different concentrations (0.5%, 1.0%, 1.5%) (with respect to PVA wt.%) was added to the cleared solution of PVA and kept the suspensions for overnight stirring at room temperature and then the suspensions were sonicated for 20 min by using probe sonicator. This process of sonication increases the solution temperature and also air bubbles were introduced in solution.

pH was measured for all prepared membrane solutions by pH paper and shown in table 4;

Table 4: pH of Membranes solution with respective PVA/Am-CNC

Membrane	PVA	Wt.% of Am-CNC (w.r.t PVA)	pH of membrane casting solution
Pure PVA	2g	Nil	6
0.5 wt.% Am-CNC/PVA	2g	0.5%	9
1 wt.% Am-CNC/PVA	2g	1%	10
1.5 wt.% Am-CNC/PVA	2g	1.5%	10

Therefore, for producing defect-free film, sonicated suspensions were kept standing for 2hr at room temperature before dip coating. The prepared suspension of PVA and aminated CNCs must be used for casting within 12hr. figure 15 shows the block flow diagram for solution preparation;

3.4. Membrane Fabrication

According to this research work demand, there are two types of the membrane were needed to cast.

- Self-support membrane, this membrane was cast for characterization.
- Supported membrane, in which membrane cast on PSF support, was used for permeation testing of CO_2.

Following are the method used for casting these membranes;

3.4.1. Self-supported Membrane Fabrication

For the self-supported membrane, the suspension was cast in Petri dishes and kept for drying at ambient temperature for 1 week. The same amount of solution was added in Petri dishes to obtained membrane film of equal thickness. Rate and time of drying for membrane were must keep constant. Membranes obtained were stored in a desiccator at RH of 0% before characterization.

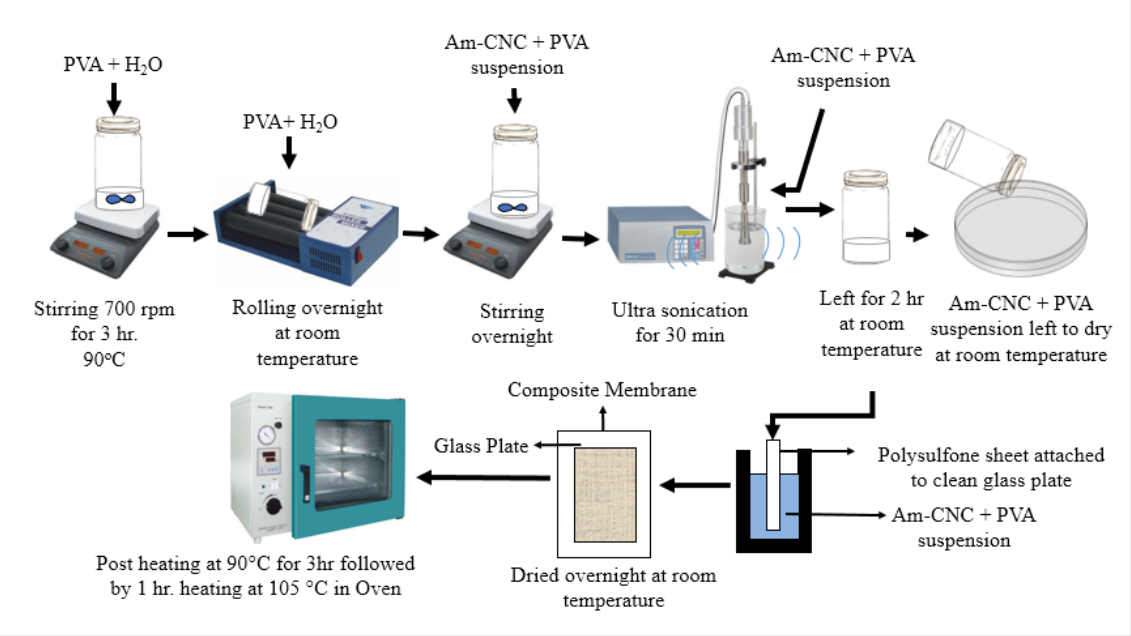

Figure 16: Flow Diagram for Solution Preparation and nanocomposite membrane fabrication

3.4.2. Pretreatment of PSf Support Layer

Before casting membrane on some support layer, pretreatment of the PSf support layer was done. There was a protective layer of polyethylene glycol coated on the upper layer of the porous PSf support membrane. So, before using the PSf support, the protective layer must be washed from surface. Therefore, standard method of washing described by Alfa Laval was followed.

The PSf membrane was cut in desired sized and with aluminum tape, these PSf membranes are attached to the glass plates. The glass plate was then placed in a constant temperature water bath at 45°C for 1hr. The same process was repeated again one more time. After that, the sheet was washed with distilled water and dried in fume hood for 30 min.

The washed PSf sheet was again cut in desired small size and attached to the small glass plates with the help of aluminum tape. So, the pretreated PSf sheet was ready for dense layer coating. The pretreated PSf sheet was not touched on surface to avoid damage to support. PFS support was used as fresh as possible to avoid the rupture of its porous.

3.4.3. Supported FTM Membrane Fabrication

The special dip coating apparatus was designed for dip coating purposes. The sonicated solution of PVA and aminated CNCs was put with the slow speed in a dip coating apparatus to avoid the air bubble formation. The solution was kept standing for 15 min to remove any air bubble if formed.

PSF support membrane attached on glass sheet was slowly dipped in the solution at dipping speed of 1.5 cm/sec. 20 sec was the approximate residence time of the PSF sheet in solution. It was ensured with aluminum tape that no solution was penetrated to the back of sheet. After 20sec, the plates were removed from solution and kept vertically for drying for 3hr in a fume hood. Then after 3hr the plates were rotated at 180^{o} angle and repeated the same procedure. The fig 17 shows the dip coating apparatus and membrane attached to glass slab.

Figure 17: Dip Coating Apparatus and Membrane Attached to Glass Slab

The dip-coated membranes were finally kept for overnight drying at room temperature in fume hood. The coasted membrane was also not touched on surface to avoid damage to the membrane. The membrane dried overnight at room temperature was then faced with heat treatment. ethylenediamine was placed in a Pre-heated oven at 45^{o}C for 3hr than

followed by 105°C for 1hr and finally, the membranes were coaled done at room temperature. The obtained membranes were ready for permeation testing.

3.5. Characterization of CNCs and membrane and membrane testing

3.5.1. Fourier Transform Infrared (FTIR) Spectroscopy

FTIR is an analytical technique that is used for the detection of the functional group present in material and also used for quantitative as well as qualitative analysis of the material. It tells us about the chemical bound present in molecules, molecular structure and the functional group present in a sample. The infra-red beam is used in FTIR, when this beam incident to sample, the sample absorbed it.

There are different energy states in sample. So, by absorbing energy from infra-red, the molecule jump from lower energy state to higher state. The different wavelength rays absorbed by these molecules is directly proportional to its transformation b/w energy states. Different functional groups absorb rays of different wavelength which is called its fingerprint. These all absorbed peaks combine together give us a complete spectrum of material. Figure 18 shows the FTIR schematic diagram;

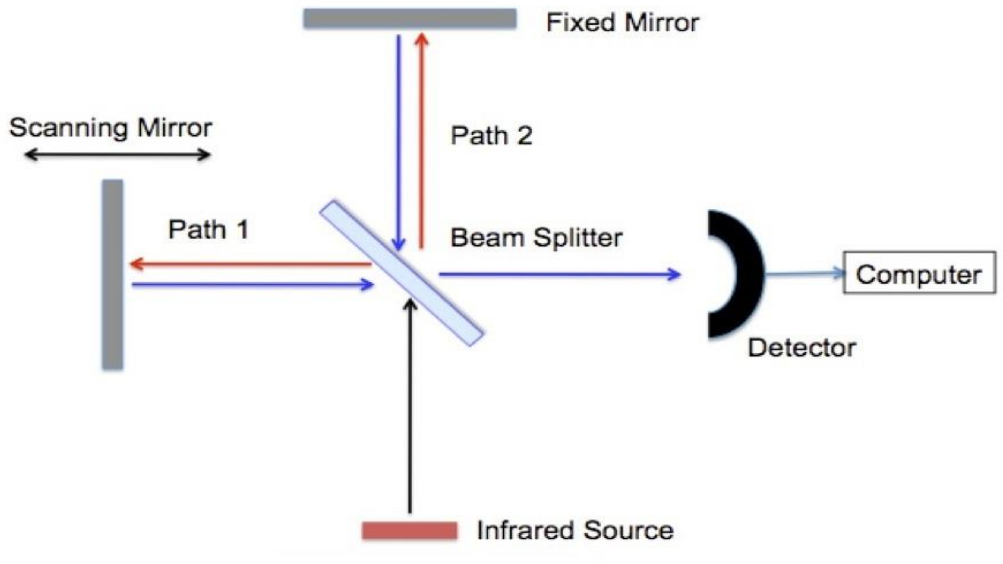

Figure 18: Schematic Diagram of FTIR Spectroscopy [91]

Spectrometer model Perkin-Elmer Spectrum 100 FT-IR was used at wavenumber range from 4000-400 cm^{-1} with a resolution of $4cm^{-1}$. First of all, pallets of KBr (potassium bromide) were prepared and then sample of aminated CNCs was placed on the pellet and subjected to the IR radiations. While sample of membranes was directly fit in the sample cell and subjected to IR radiation. Different functional groups that are present in sample were studied.

3.5.2. X-Ray Diffraction

In this analytical technique, the dual nature of x-ray i.e. particle and wave nature both are used to get the exit picture of crystalline structure. This technique is used to identify and characterize the compounds present in a sample. It helps in finding the following properties in the sample; phase purity, shape, and size of crystallites, lattice parameters, and crystallinity.

For calculating crystallinity from XRD graphs, origin software was used to calculate the total area under the crystalline peaks and total area under the diffraction curve (both crystalline and amorphous), by using following equation;

$$\% \text{ Crystalinity} = \frac{\text{Area under the crytaline peaks}}{\text{Total aera under the the diffraction curve}}$$

There are three major components in X-ray diffractometer; x-ray tube, sample holder and an x-ray detector. The cathode x-ray tube is used for generating an electron to produce an x-ray. Then by applying potential differences, electrons are accelerated. Then these electrons are bombarded on a targeted material like copper. So, outer most electrons are knocked out from the copper produced an x-ray. These x-rays are then bombarded on the sample. The rays which are reflected from the sample are detected on a detector. Their intensity is recorded and studied. Bragg's law is used for identifying d-spacing between two layers of any structure at any given angle. It also gives help in understanding diffraction phenomena and also crystal diffraction. Bragg's law is given as;

$$n\lambda = 2d\sin\theta$$

Figure 19 shows the schematic diagram for X-ray diffractometer;

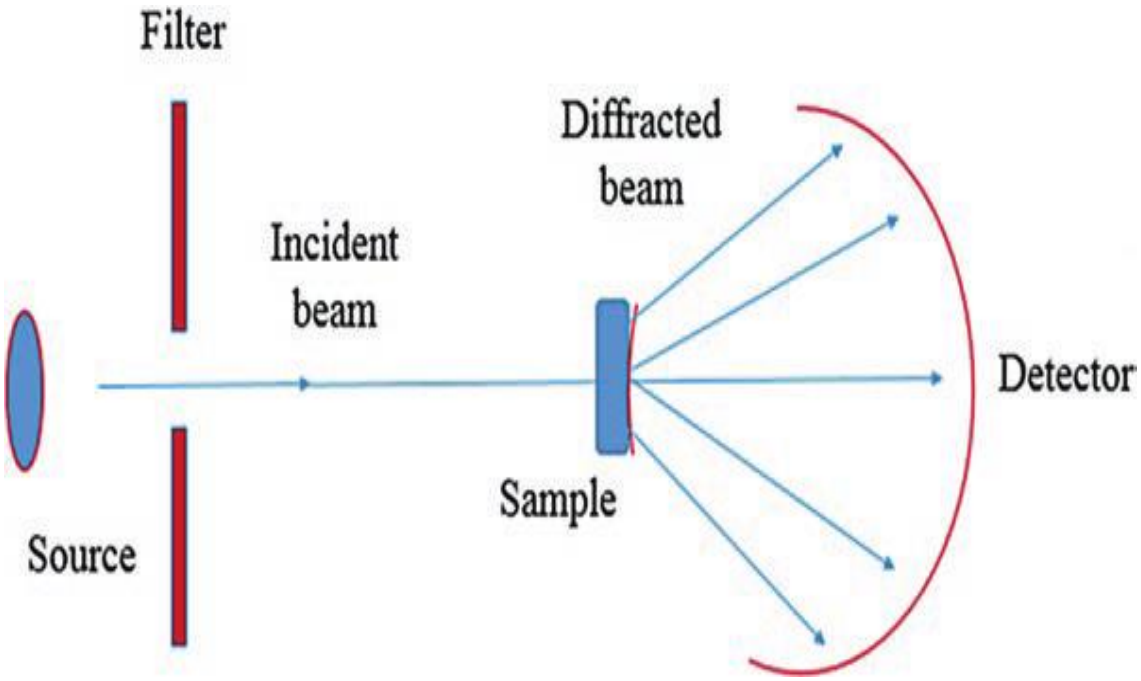

Figure 19: XRD Schematic Diagram [92]

STOE X-ray Diffractometer was used for analysis in this research. The crystallinity index of aminated CNCs and Nanocomposite membrane samples was determined. Scan angle was set b/w 10 to 40^{o} with a step size of 0.4^{o} and step time of 1. Cu K α-1 was used as radiation energy for x-ray diffraction while frequency used was 1.5406 Å. The membrane's crystallinity index was determined by method followed in literature. total area was the area under the curve of XRD spectrum b/w 10 to 40^{o} [93].

3.5.3. Scanning Electron Microscopy (SEM)

This analytical technique is used for studying the following characteristics of Nanocomposite membrane; surface morphology, topography, cross-section structure of Nanocomposite membrane, crystalline structure and their pores geometry. Following are the basic component of SEM;

i. Source for electron generation
ii. A column with electromagnetic lenses in which electron moves.
iii. Electron detector
iv. Sample chamber
v. Screen or computer for image display.

In SEM, the electron beam is fired on the sample. So, when it incident to the surface of the sample, it examined all desired characters of specific areas of sample with much accuracy. When the electron beam falls on surface of sample, a single is generated which is received to the detector and analyzed and show image on the screen. Figure 20 gives the schematic diagram of SEM;

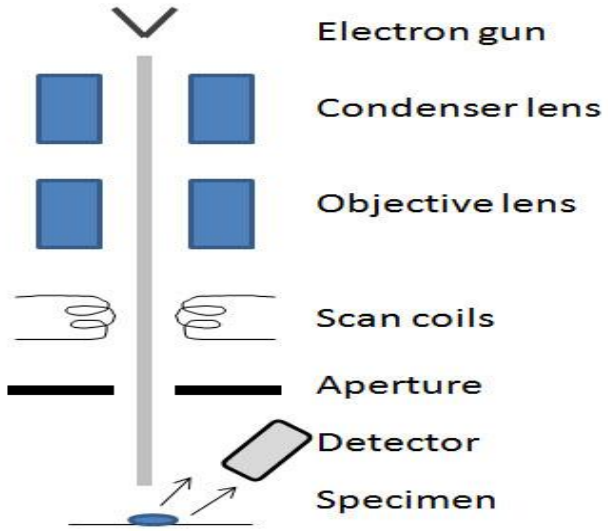

Figure 20: SEM Schematic Diagram [92]

SEM of model S-4700 Hitachi, Japan was used for SEM analysis of Nanocomposite membrane samples. While the ion sputtering machine of model JFC-1500 of JEOL Ltd was used for gold sputtering on sample. Image magnification was taken from range of 500x to 10,000x with voltage of 5Kv. Surface and cross-sectional images of Nanocomposite membrane were taken. For cross-sectional image, the liquid nitrogen was used for cracking samples to calculate the thickness of the dense membrane.

3.5.4. Moisture Uptake or Swelling Test

In this test, the swelling behavior of PVA and aminated CNC based Nanocomposite membranes were examined at room temperature under humid condition. For this test, a sample of membranes was placed at 0% relative humidity in a closed chamber. Then the humidity of the chamber was increased to 87% by using concentrated solutions of following salts. Each salt has its own relative humidity like 33% RH for magnesium chloride, 75% RH for sodium chloride and 97% RH for potassium sulfate [94]. By placing

membrane in humid condition, the humidity of chamber decreased because of moisture absorb by membrane, the equilibrium was maintained in chamber by forward reaction of salts to maintain the RH at 87%.

There was no direct contact of membranes samples to the solution in a chamber. Reading was taken after each 24hr, by measuring the weight increased of membranes sample to calculate degree of swelling. The process of weight measuring was repeated for ten days to measure the slight change in weight until the reading became constant. The reading was taken from first day at 0% RH to 87%RH. The equation used for calculating degree of swelling is given below.[94].

$$\mathrm{DoS} = \frac{\alpha' - \beta'}{\beta'} \mathrm{X}\ 100$$

Where α' is used for swelled membrane mass and β' is used for dry membrane mass respectively. Figure 21 given below shows the setup for the swelling test.

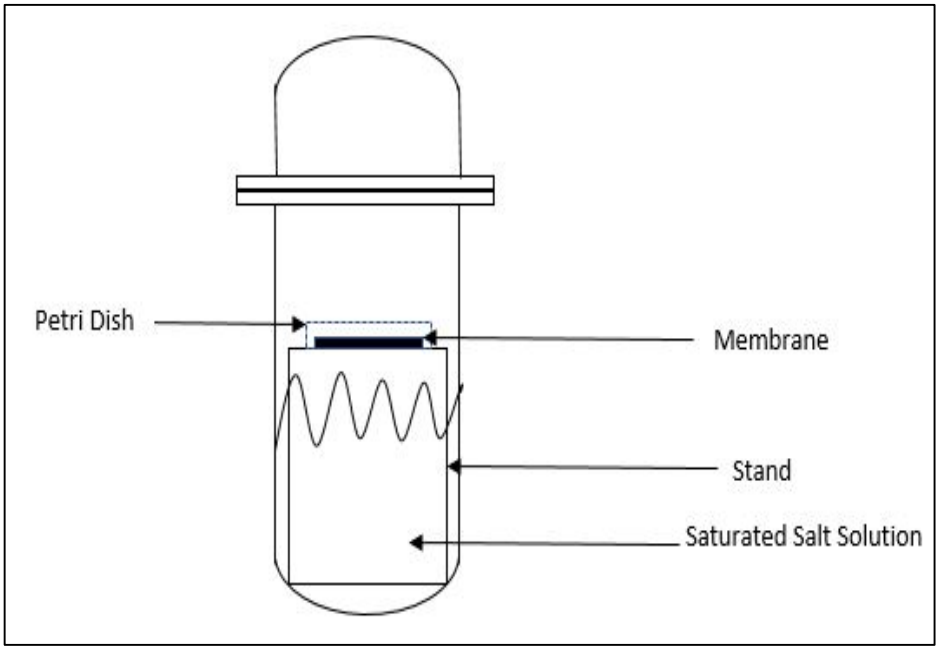

Figure 21: Setup for Swelling Test

3.5.4. Gas Permeation Test

The gas permeation across the membrane was calculated through the proper gas permeation system. In this system, permeation rig made of stainless steel with high-

pressure bearing ability up to 20bar was used for finding the permeance of gas across the membrane. Membrane rig based on high pressure was designed product technology lab of NUST University. Following equation is used for calculating the permeability of gas across the membrane;

$$P = \frac{q.l}{A.\Delta P}$$

Where,

P = Permeability express in the barrer unit.

1 barrer $=10^{-10}$. cm^3(STP). cm. $cm^{-2}.s^{-1}$. cm Hg^{-1}

Q = Flow rate of permeate across the membrane (cm^3/s)

L = Thickness of the membrane (cm)

A = Active area of membrane (cm^2)

ΔP = Pressure difference between P1 and P2 at feed and permeates side. (cm of Hg)

While selectivity for gases can be calculated by the following equation;

$$\alpha_{\frac{A}{B}} = \frac{PA}{PB}$$

In this testing, the separation performance of Nanocomposite membrane based on PVA and aminated CNCs was tested. So, membrane sample was fitted in a membrane cell. Nitrogen as a sweep gas was introduced in a system at room temperature and low pressure. Nitrogen gas was first pass through a humidifier containing water, nitrogen carries some water molecule with his self and inter in a membrane cell, where it sweeps over a membrane surface, membrane absorbs water molecules from gas while the used gas was exhausted.

After 3days of sweeping nitrogen gas on membrane surface, the maximum swelling was achieved. After swelling the permeation test for feed gases (CO_2 and CH_4) was conduct for which both gases one by one introduced from the top of membrane cell and reading

for flow rate of CO_2 and CH_4 were taken with the help of bubble flow meter at different pressures i.e. 5, 10 and 15 bar for different concentration based membranes samples like 0.5, 1.0 and 1.5wt% concentration.

The calculated flow rate of gas, the thickness of dense layer, active surface area of membrane and pressure difference, all values were added in an above-given permeability formula to calculate the permeability of both gases. Figure 22 shows the flow diagram for the high-pressure permeation testing system.

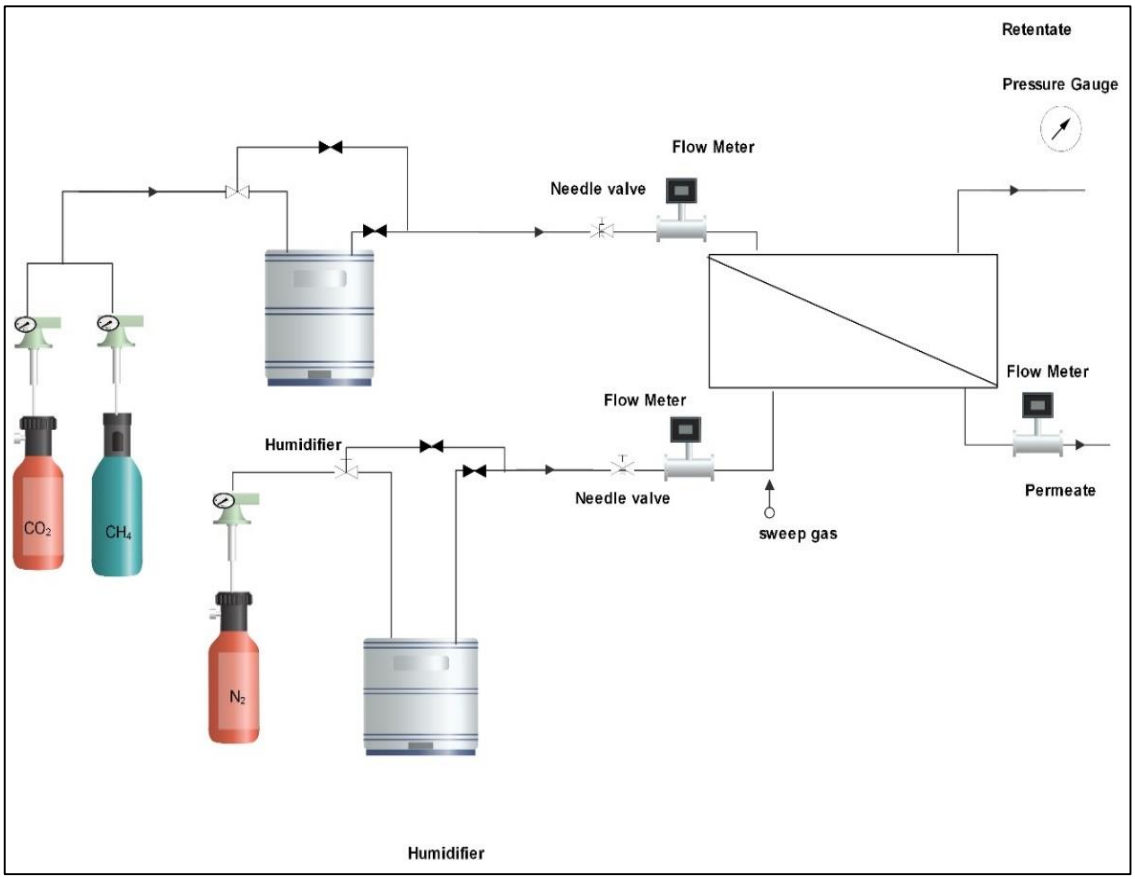

Figure 22: Flow Diagram for the High-pressure Permeation Testing System

Chapter 4

Results and Discussion

4.1 Characterization Techniques

The characterization techniques used for the analysis of membrane properties are following;

- FTIR spectroscopy, used for the examination of amine functional group attachment to CNCs and different functional groups present in membranes.
- XRD, used for the examination of the crystalline nature of filler and membranes.
- SEM, used for the examination of surface morphology and cross-sectional analysis of membrane.

4.2. Analysis Through FTIR Spectroscopy

The spectra of FTIR for pure Cn, Am-CNC, PVA and PVA/Am-CNC composite membranes for varying concentration of aminated CNCs are given in figure 23. There are typical bends for cellulose in both spectrums of CNC and aminated CNC while there is very little difference between the characteristic peak spectrum of neat PVA and nanocomposite membrane of PVA and aminated CNC.

The band appeared around 3409, 3419 in nanocomposite membranes and 3435 cm^{-1} in pure PVA while from a range of 3291-3350 cm^{-1} [95] in CNC and aminated CNC are O-H stretching vibration from intermolecular hydrogen bonding within PVA, CNC and aminated CNC and in their Nanocomposite membranes . While the peaks range from 3050-2800 cm^{-1} in CNC, aminated CNC and nanocomposite membranes are for C-H band stretching vibration of CH_2 and CH_3 groups [96]. The –CH, C–C and C–O bend stretching appeared at 1361, 1316 and 1161 cm^{-1}, respectively in aminated CNC and nanocomposite membranes [97]. The band at 894 and 885 cm^{-1} are for CH out-plane bending in CNC, aminated CNC and nanocomposite membranes. A strong absorption peak at 1645 cm^{-1} in CNC sample, 1635 cm^{-1} in PVA sample and 1622 cm^{-1} in the

Nanocomposite membrane is for O–H bending vibration of water absorbed by the cellulose, PVA and nanocomposite membrane [98].

From these results, it is concluded that amine-modified CNC maintained the internal structure of cellulose after the modification, heating processes and in nanocomposite membranes based on PVA and aminated CNC [99]. Two new peaks appeared in aminated CNC and Nanocomposite membrane based on PVA and aminated CNC at 1587 and 1471 cm^{-1} is for N–H bend stretching of the NH_2 group which gives the conformation of amine group attachment to CNC [57].

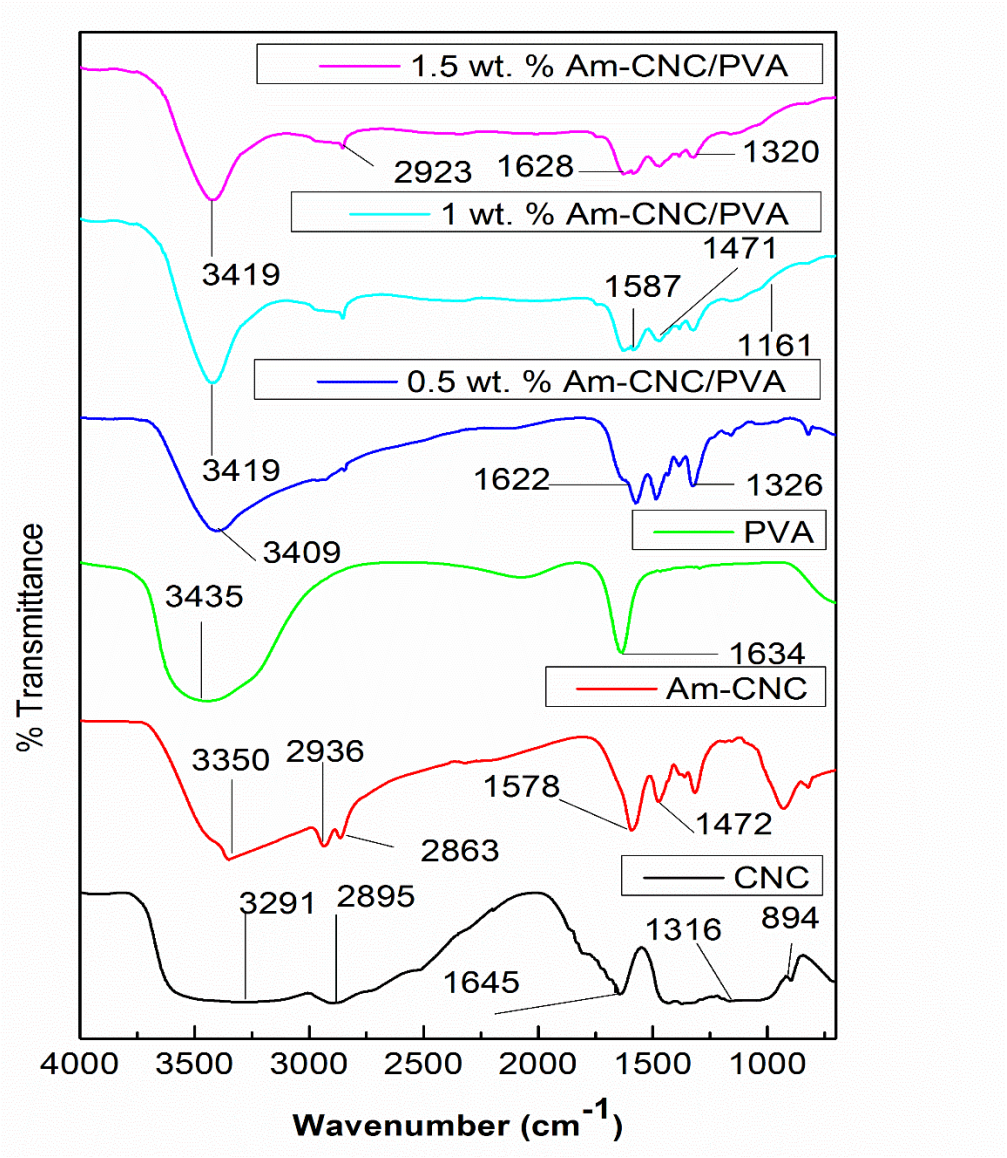

Figure 23: FTIR spectra for CNC, Aminated CNC, PVA and PVA/Aminated CNC Based Nano Composite Membranes

4.3. X-ray Diffraction Results

Figure 24, shows the XRD pattern of CNC, Aminated CNC, pure PVA and PVA/Am-CNC membranes.

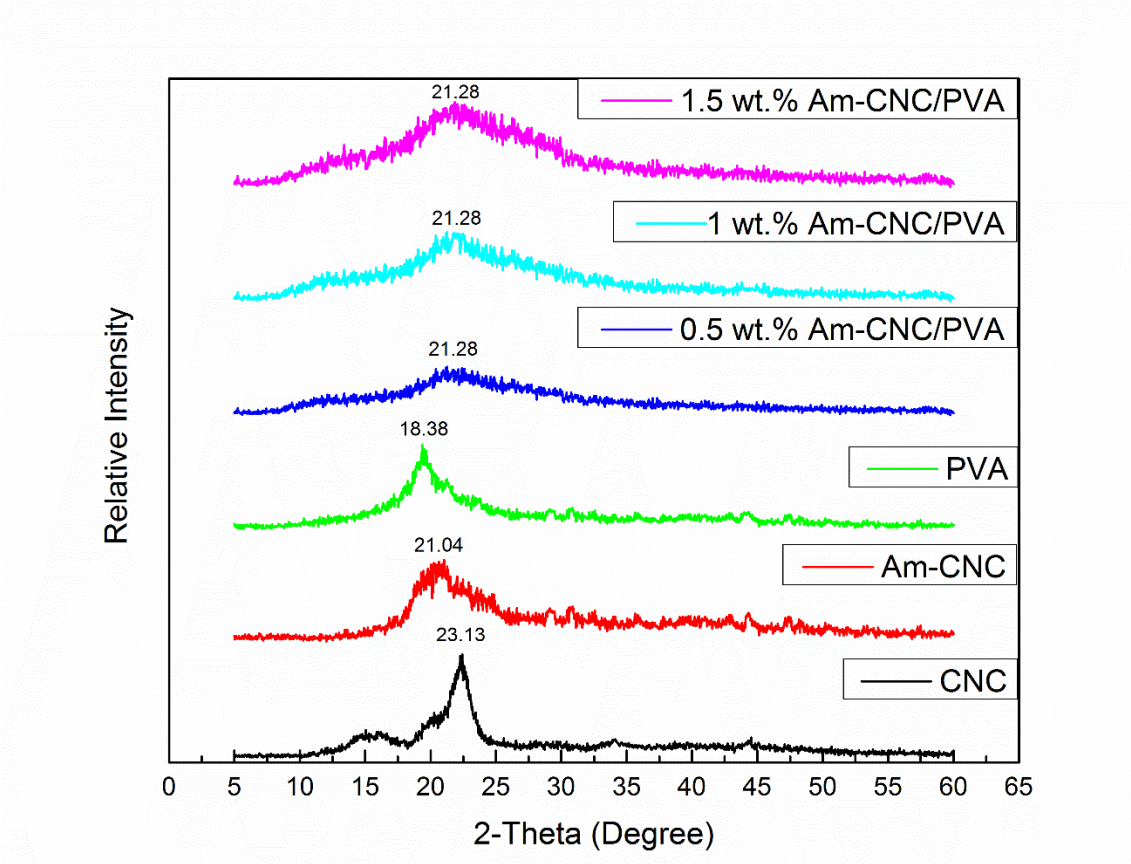

Figure 24: XRD Spectra of Pure CNC, Am-CNC, PVA and PVA/Am-CNC Based Nanocomposite Membranes

The crystallinity of CNC, Am-CNC, pure PVA and PVA/Am-CNC composite membranes were calculated from a graph. Pure CNC showed a sharp peak at $2\theta = 23.13^{O}$ with crystallinity up to 64% while Aminated CNC peak was shifted to 21.04^{o} with decreased in intensity of peak which shown that the crystallinity of Am-CNC was decreased with value of 58%. The pure PVA membrane showed a sharp peak at $2\theta = 18.38^{O}$. The crystallinity for pure PVA membrane was calculated to be approximately 53%. When 0.5 wt.% Am CNC was added to PVA matrix. The PVA and Am-CNC peaks lies near to each other so their peaks overlap with each other having single bold and sharp

peak at 21.28°. The intensity of PVA remains constant without any major change, while intensity of peak in composite membranes was change due to increasing concentration of Am-CNC. The 0.5 wt.% Am-CNC in PVA based composite membrane had shown more crystallinity than pure PVA based membrane with a value of approximately 58.7%. Moreover, it was seen that if concentration of Am-CNC increased in PVA matrix, crystallinity of composite membranes also increased. The addition of Am-CNC shows only change in intensity while did not cause any peak shift. Moreover, the composite membranes crystallinity has directly proportional to Am-CNC concentration. The crystallinity at 1wt.% Am-CNC based composite membrane was calculated up to 60.67%. Figure 25 shows the effect of CNC concentration on % crystallinity of the membranes.

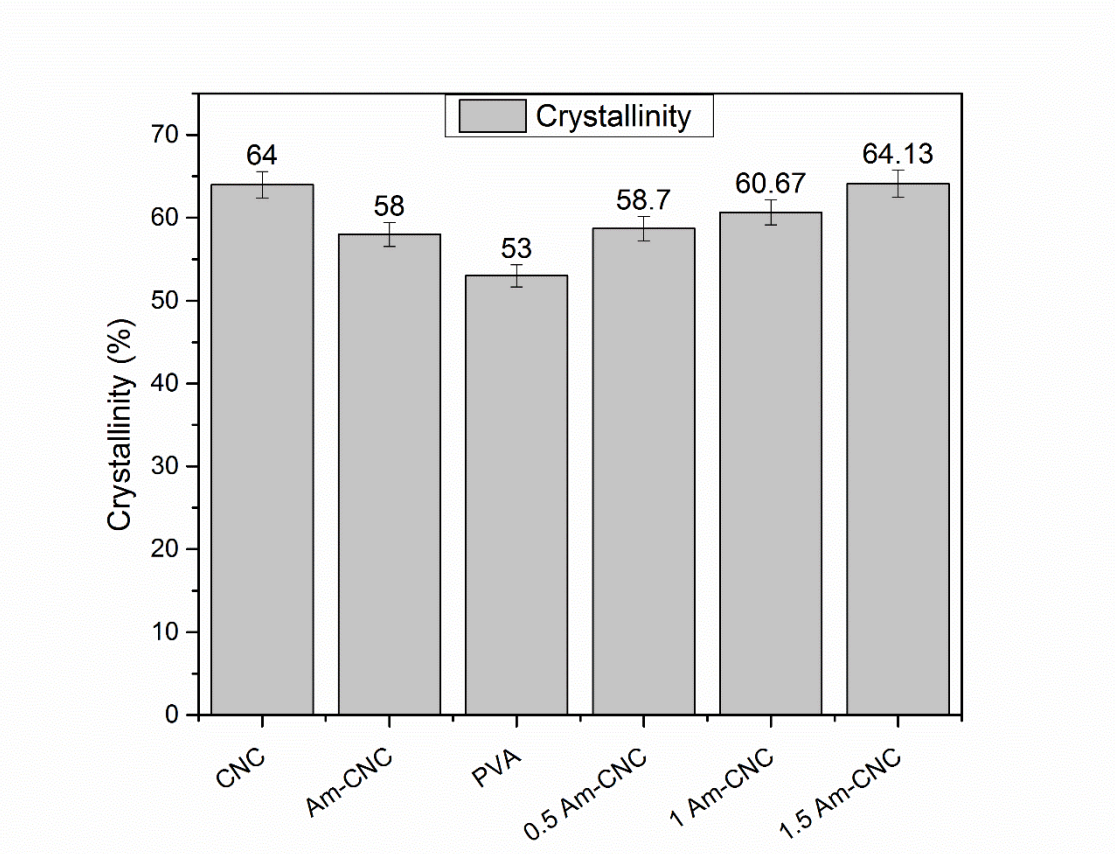

Figure 25: Crystallinity of CNC, Am-CNC, PVA and Am-CNC Concentration vs % Crystallinity

The maximum crystallinity was shown by the composite membrane which had an Am-CNC concentration of 1.5 wt.% i.e. 64.13%. The amorphous area of Polymeric matrix decreased with increasing the crystalline nature of the composite membranes. Increasing crystallinity increased the rigidity in polymer so decreased the mobility of the polymeric chains which affect the separation performance of the composite membranes. Moisture uptake by membranes make rearrangement in molecular domains, due to which crystallinity increased. However, chain flexibility of the polymer matrix was increased due to water in water-swollen membranes. So, the best separation results are expected for membranes at high relative humidities with optimum Am-CNC concentration [56, 90]. Figure 18 shows the CNC concentration effect on % crystallinity of the membranes.

4.4. Degree of Swelling / Moisture Uptake Result

Moisture uptake of PVA/Am-CNC based nanocomposite membranes was studied by placing them in a humid condition with RH of 87%. The Am-CNC played basic role in moisture uptake in these. Figure 26 shows the maximum moisture uptake result for 10 days' period.

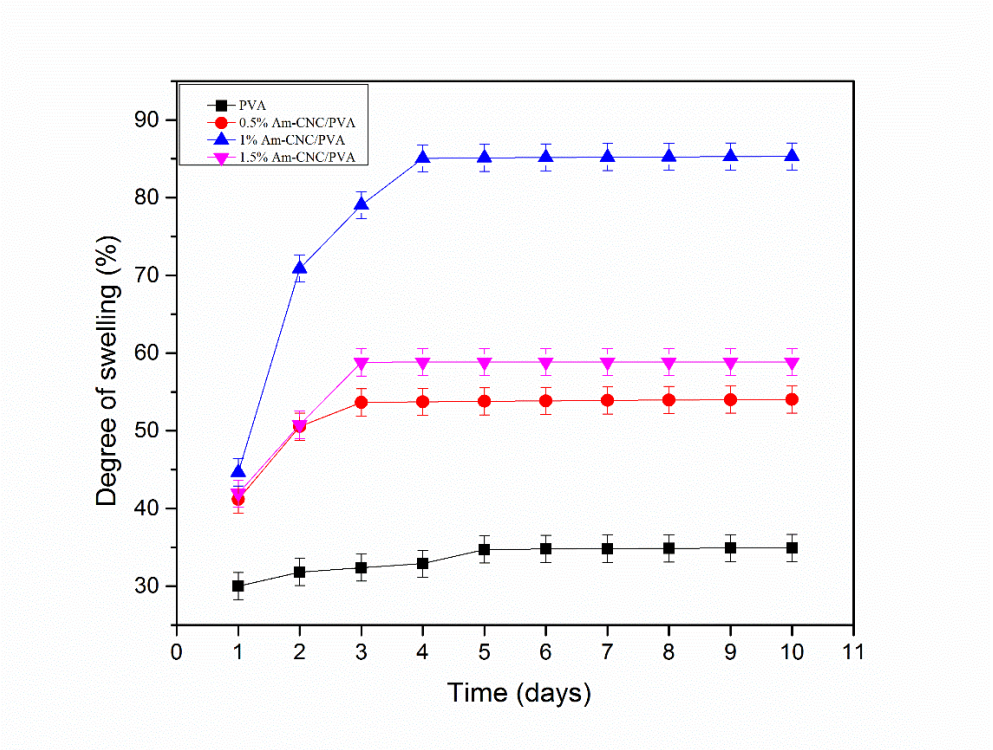

Figure 26: Degree of Swelling for Formulated Membranes

The maximum moisture uptake was observed until day 4 (figure 27), but the membrane has 1% Am-CNC concentration, absorbed the moisture till day 4 as shown in figure 27.

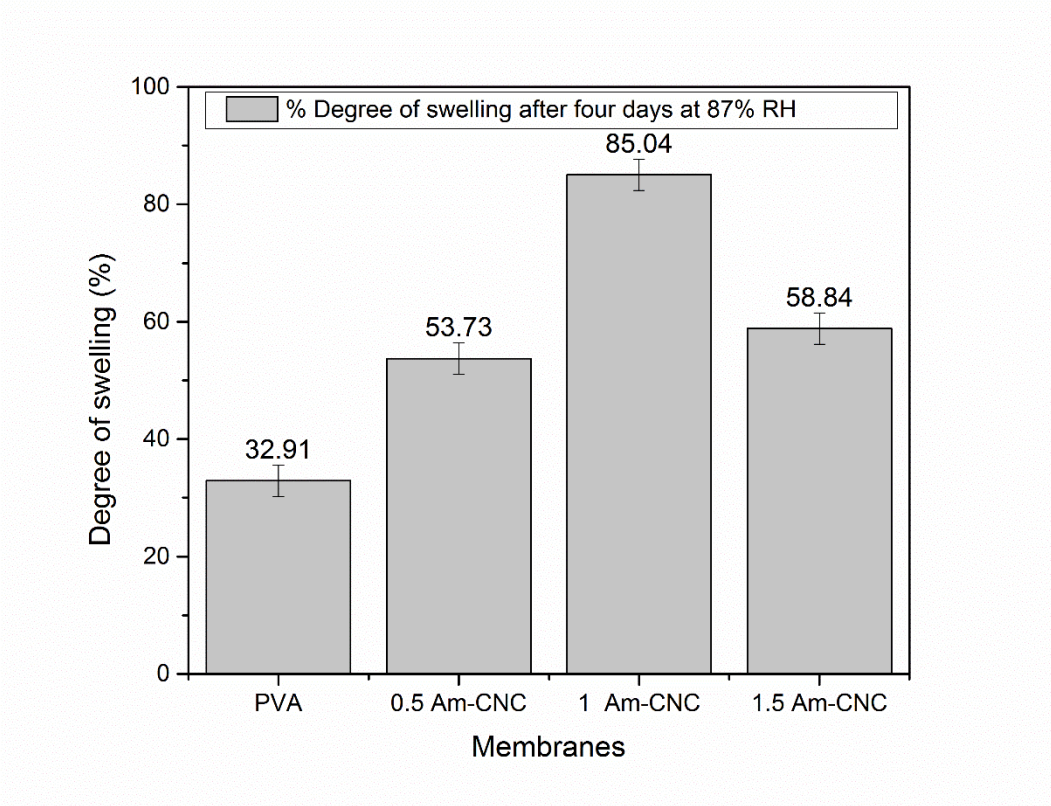

Figure 27: Maximum Degree of Swelling After 4 Days

Furthermore, in the case of pure PVA membrane, the continues and gradual increase in moisture uptake was noted till day 5 and 6. 0.5 and 1.5 wt.% Am-CNC concentrated membrane shows sharp increase in degree of swelling till day 2 then gradual increase till day 3 after that degree of swelling became almost constant. 1% wt. Am-CNC concentrated membrane shows sharp increase in degree of swelling till day 2 then gradual increase till day 4 after that the degree of swelling became almost constant.

85.31% was the maximum degree of swelling observed for 1% wt. Am-CNC concentrated membrane, while membrane with 1.5 wt.% Am-CNC shown degree of swelling 58.84%, the reduction in moisture uptake with increasing concentration of Am-CNC because CNC molecules have strong reinforcement capability. This property makes

resistance to the mechanical restraining of CNC molecules and the further moisture uptake was rejected. Its cause to decrease the degree of swelling in nanocomposite membrane based on PVA/Am/CNC. So, as the Am-CNC concentration increases, the crystallinity index of membrane also increases as discussed above, which reduces the moisture uptake ability of membranes. Higher the moisture uptake ability higher will be the CO_2 separation ability of membranes. So, higher CO_2 permeation was calculated at high RH with optimal concentration of Am-CNC in PVA based nanocomposite membranes [54, 56, 90].

4.5. Scanning Electron Microscopy (SEM) Results

The surface and cross-section morphology of the membrane was examined with field emission scanning electron microscopy. The figure 28 (a), 28 (b), 28 (c) and 28 (4) show the surface images for Pure PVA, 0.5 wt.% Am-CNC/PVA, 1 wt.% Am-CNC/PVA and 1.5 wt.% Am-CNC/PVA.

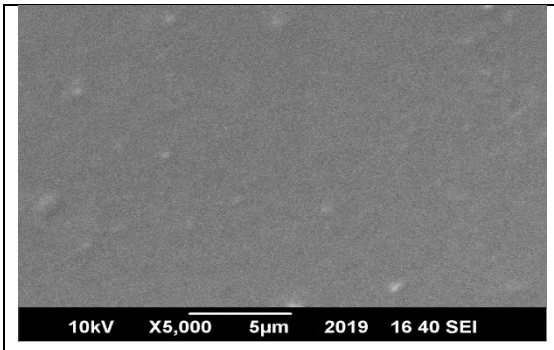

Figure:28(a)

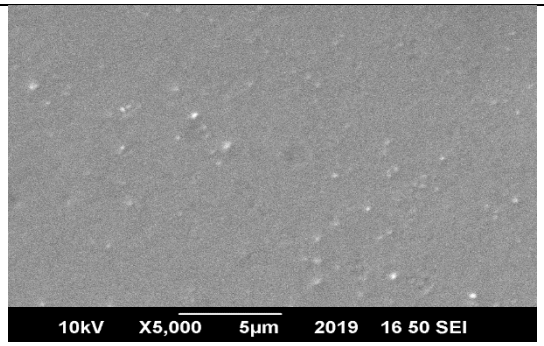

Figure:28(b)

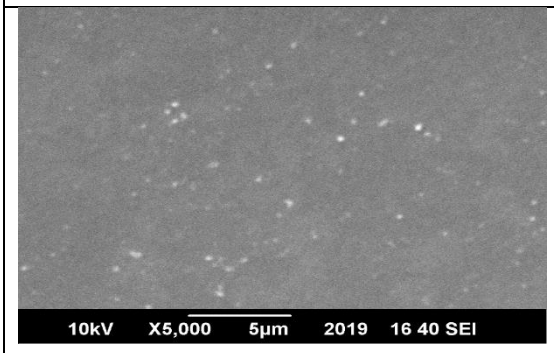

Figure:28(c)

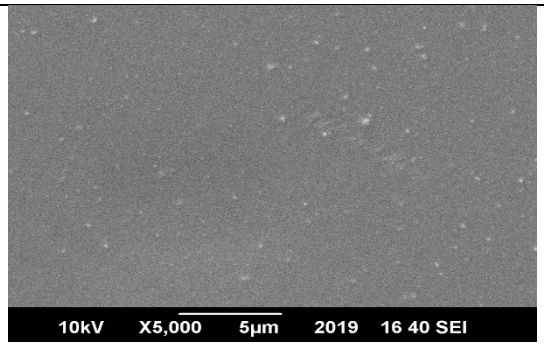

Figure:28(d)

Figure 28: Images showing surface morphology of nanocomposite membrane for (a) Pure PVA membrane, (b) 0.5 wt.% Am-CNC/ PVA Membrane, (c) 1 wt.% Am-CNC/ PVA Membrane, (d) 1.5 wt.% Am-CNC/ PVA Membrane

In Fig. 28 (a), smooth and defect-free surface image of the PVA membrane is shown while Fig. 28 (b) shows the surface image of nanocomposite membrane containing 0.5% Am-CNC which was shown in imbedded form on membrane surface.

Fig. 28 (c) and Fig. 28 (d) also shows the surface morphology of nanocomposite membranes containing 1% Am-CNC and 1.5% Am-CNC in embedded form respectively. As the concentration of Am-CNC increases the amount of imbedded particles on surface also increases [56, 90].

Fig. 29 (a), Fig. 29 (b), Fig. 29 (c) and Fig. 29 (d) shows the cross-sectional view of PVA membrane cast on PSf support and nanocomposite membranes with 0.5% Am-CNC, 1% Am-CNC and 1.5% Am-CNC cast on PSf support. From different parts of each composite membranes, samples were taken and readings were taken for each sample respectively.

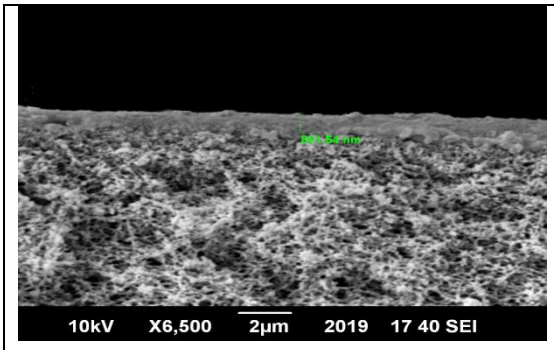

Figure:29(a)

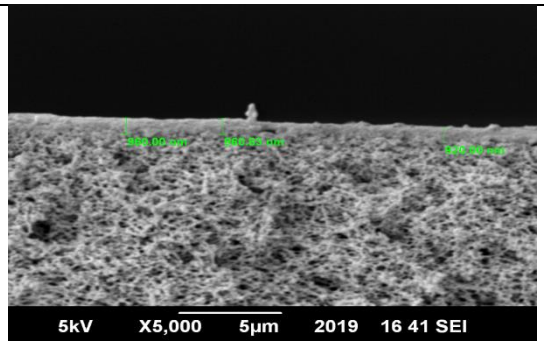

Figure: 29 (b)

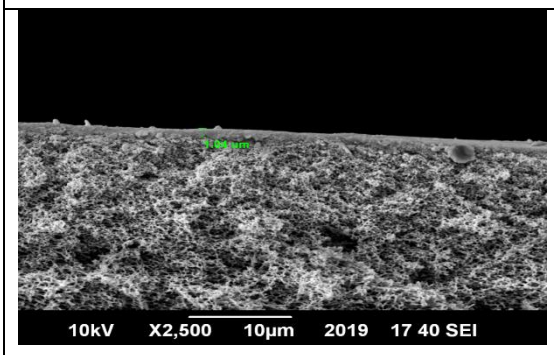

Figure: 29 (c)

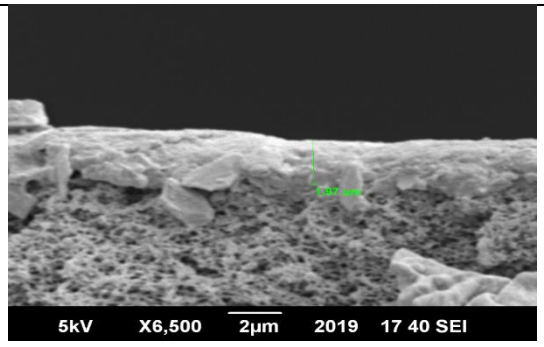

Figure: 29 (d)

Figure 29: Images showing cross- sectional of nanocomposite membrane for (a) Pure PVA membrane, (b) 0.5 wt.% Am-CNC/ PVA Membrane, (c) 1 wt.% Am-CNC/ PVA Membrane, (d) 1.5 wt.% Am-CNC/ PVA Membrane

The average thickness which was observed for the selective layer of PVA membrane was 886 nm. While, average thickness observed for selective layers of 0.5 wt.% Am-CNC/PVA, 1 wt.% Am-CNC/PVA and 1.5 wt.% Am-CNC/PVA composite membranes are 940, 1040 and 1970 nm respectively. It was noticed that when Am-CNC concentration increased will increased the thickness of the selective layer.

In figure 30, thickness variation with increasing Am-CNC concentration was shown. Increasing trend in thickness of dense layer of composite membranes is because of viscosity of the casting suspension, which also increased with Am-CNC concentrations increasing which give higher suspension thickness on the support after dip-coating [56, 90].

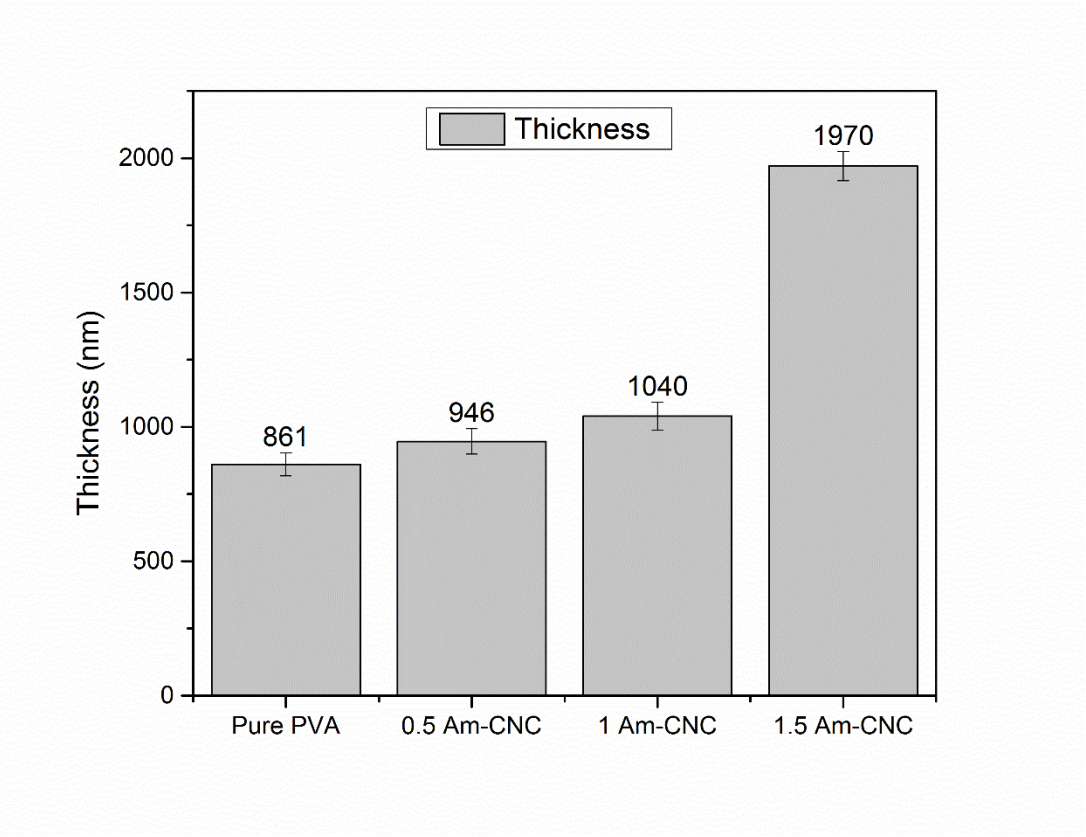

Figure 30: Shows a Graphical Representation of the increasing Am-CNC Concentration effect on Thickness of Selective Layer of Membranes

4.6. Permeation Testing

Single gas permeation testing for nanocomposite membranes based on PVA/Am-CNC having Am-CNC concentration of 0.5, 1, 1.5 wt.% (w.r.t PVA concentration) was carried out at 5, 10, 15 bar. the results of permeance and selectivity was discussed below in detailed.

4.7. Am-CNC Concentration effect on CO_2 and CH_4 Permeation

4.7.1. Am-CNC Concentration effect on CO_2 Permeance

The Am-CNC concentration effect on the permeance of CO_2 is shown in figure 31 below. From above figure it was observed that the permeance of CO_2 in pure PVA membrane was very low as compared to the composite membranes based on PVA/Am-CNC. It means that adding Aminated CNC as a filler in a PVA had positive effect on permeance of CO_2 across the membrane. The swelling effect of PVA membrane improved by adding Am-CNC because CNC has the ability to absorb water molecule, these water molecules help in facilitated transport while on other hand it was also noticed from the results that the amine functional group attached to CNC also improved the facilitated transport of CO_2 across the membrane while the CH_4 molecule have inert nature, show no reaction with amine group or water so, they follow only diffusion mechanism for transport across the membrane.

The mechanism of facilitated transport of CO_2 through unhindered amine group reaction was described by Caplow [100]. The CO_2 tends to make carbamate ion through a zwitterion mechanism shown in equation 1 and 2;

$$CO_2 + R - NH_2 \leftrightharpoons R - NH^+_2 - COO^- \quad (1)$$

$$R - NH^+_2 - COO^- + R - NH_2 \leftrightharpoons R - NH - COO^- + R - NH^+_3 \quad (2)$$

The CO_2 molecule interact with two amine groups which facilitated the CO_2 diffusion. The upstream side reaction mechanism was shown in equations. In these equations the CO_2 complexing reaction with carrier molecules (amine group), when CO_2 is dissolved was described. The de complexing reaction of CO_2 was take place at downstream side which allow CO_2 molecules once again to pass in gaseous form [100].

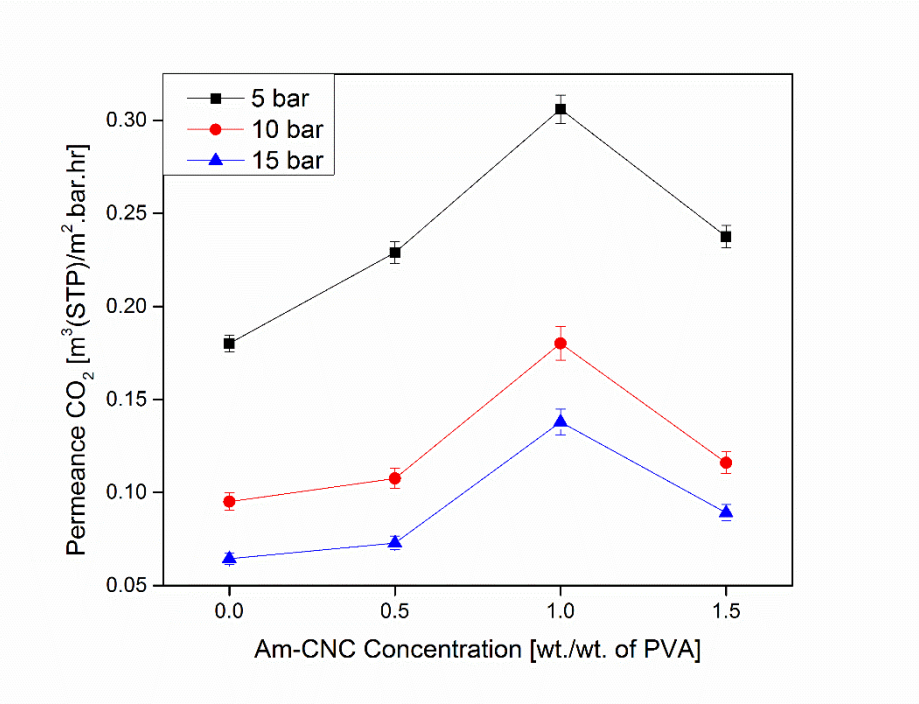

Figure 31: Am-CNC Concentration effect on Permeance of CO_2

The water molecules absorbed by membrane caused to swell up the membrane which increases the free gap volume area within a chain of polymer. These gaps help to diffused both CO_2 and CH_4 across the membrane because the molecular size of CO_2 and CH_4 is approximately same i.e. 3.3Å and 3.8 Å respectively. However, as the CO_2 solubility in water is high due to which the permeance of CO_2 also high then CH_4.

It was also observed from graph that the permeance of CO_2 in pure PVA membrane was .18009 m^3(STP)/m^2.bar.hr. The CO_2 permeance was increased till 1 wt. % Am-CNC have value of .306 m^3(STP)/m^2.bar.hr, after that permeance of CO_2 was decreased. The CO_2 permeance was dropped from .306 m^3(STP)/m^2.bar.hr to .2396 m^3(STP)/m^2.bar.hr, when concentration of Am-CNC was increased from 1 wt.% to 1.5 wt.% at 5 bar respectively [56, 90].

There are the following reasons for this which are discussed below;

- Moisture uptake capability of composite membranes was decreased by increasing the Am-CNC concentration as discussed above.
- The crystallinity of composite membranes was increased with increasing Am-CNC concentration as discussed above.

- As the concentration increased so the thickness of membranes also increased as discussed above.

4.7.2. Effect of Am-CNC Concentration on CH_4 Permeance

When CH_4 permeance across the composite membrane was studied. It was observed that increase in concentration of Am-CNC caused to gradually decreased in CH_4 permeance as given in figure 32. The reason for that is, CH_4 is inert gas so it never reacts with water molecules and amine functional group. So, by swelling, the free gaps area volume between chain of polymers increased which provide way for diffusion to CH_4 but with increasing concentration these free area volumes decreased so diffusion also decreased. The maximum permeance for CH_4 was noticed for pure PVA membrane i.e. 0.0131 $m^3(STP)/m^2.bar.hr$ with gradually decreased permeance by increasing Am-CNC concentration up to 1.5 wt.% Am-CNC the lowest value for CH_4 permeance was observed i.e. 0.00365 $m^3(TP)/m^2.bar.hr$ [56, 90].

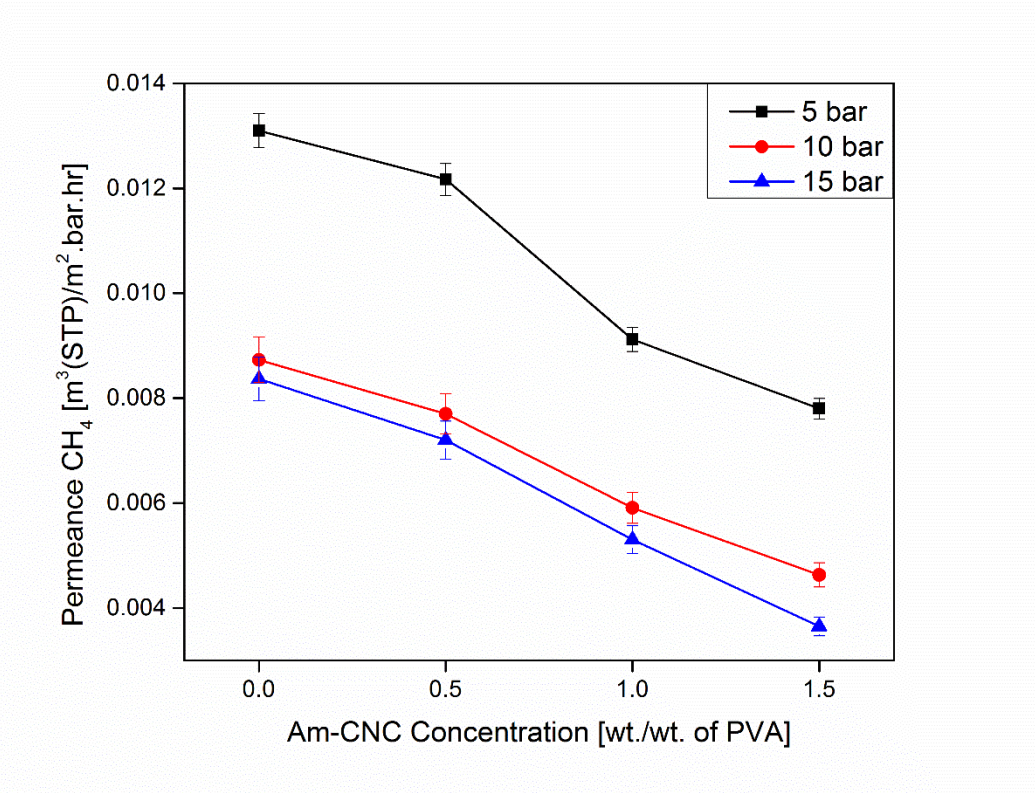

Figure 32: Effect of Am-CNC Concentration on Permeance of CH_4

4.7.3. Effect of Am-CNC Concentration on Selectivity

The selectivity trend for CO_2/CH_4 is given in figure 33. The trend of selectivity is almost the same as to the trend of CO_2 permeance i.e. the selectivity was increased up to 1 wt.% Am-CNC concentration, after that going to decrease with increasing concentration up to 1.5 wt. of Am-CNC.

The drop in selectivity is because of drop in the permeance of CO_2 and CH_4 at 1.5 wt.% concentration. The selectivity was dropped from 33.55 to 30.46 by increasing concentration from 1 wt.% to 1.5 wt.% at 5bar pressure [56, 90].

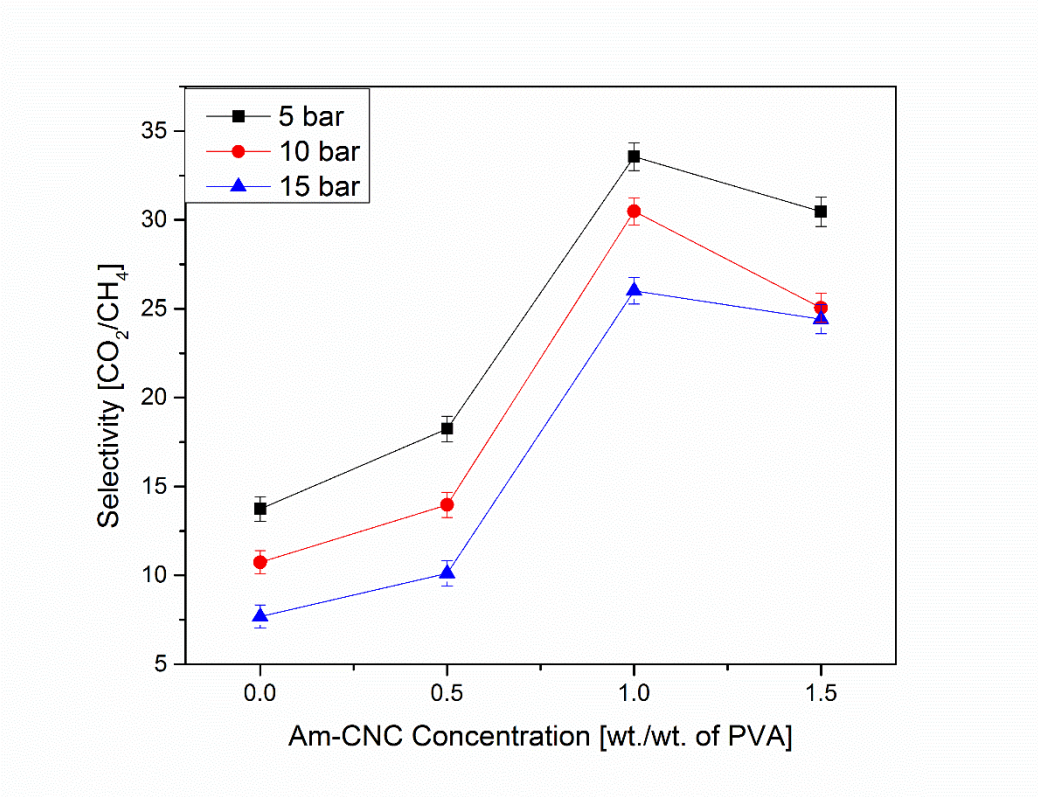

Figure 33: Effect of Am-CNC Concentration on Selectivity

4.8. Pressure effect on Permeation of CO_2 and CH_4 and Selectivity

4.8.1. Pressure effect on Permeation of CO_2 and CH_4

From figure 34, it was noticed that the effect of pressure on CO_2 permeance was in decreasing trend i.e. with increasing pressure from 5 bar to 15 bar the CO_2 permeance

was decreased. The maximum permeance for CO_2 was .306 $m^3(STP)/m^2.bar.hr$ at 5 bar for PVA/1 wt.% Am-CNC nanocomposite membrane, while minimum permeance for CO_2 was 0.06443 $m^3(STP)/m^2.bar.hr$ at 15 bar for pure PVA membrane.

There are following reasons for decreased in permeance of CO_2 with increasing pressure;

- The compaction in the size of nanocomposite membranes at high pressure. The membranes are squeezes at high pressure due to which its swelling ability reduced even at very high relative humidity.
- Loss of water molecules from membrane causes to reduce the mobility of chains of polymeric Matrix and free volume of the membrane.
- The phenomena of plasticization in the polymeric membrane due to high pressure is also caused by reduction of CO_2 and CH_4 permeance [90].

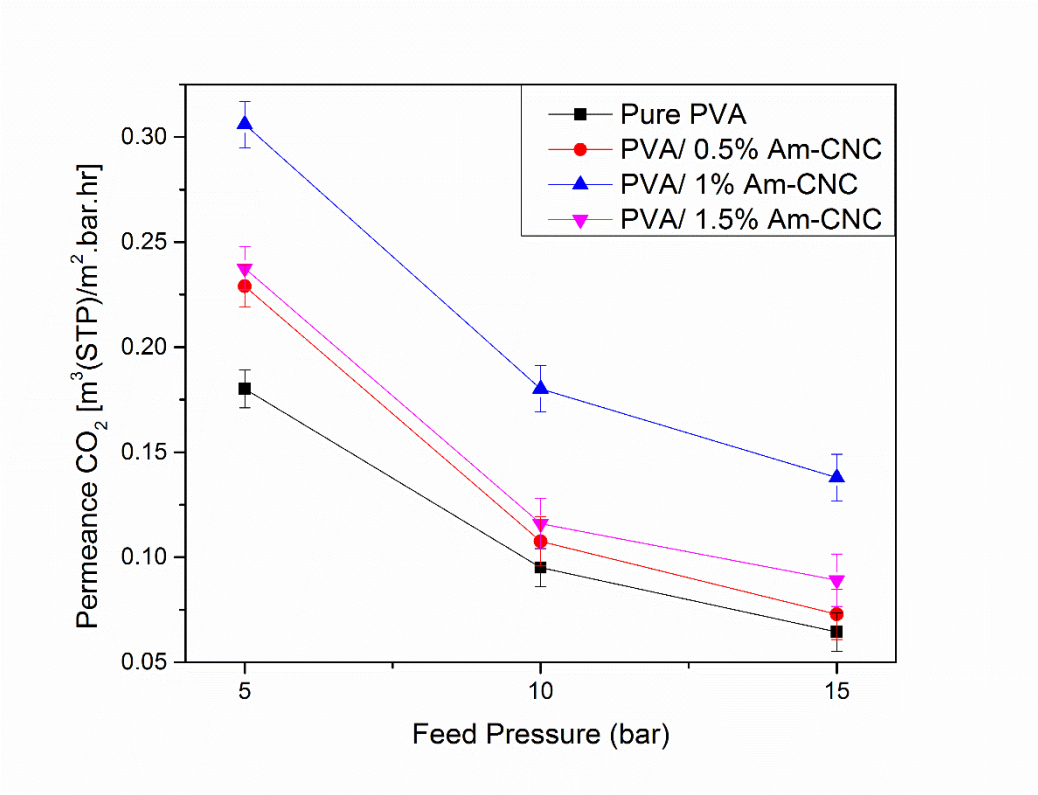

Figure 34: Pressure effect on Permeance of CO_2

When CH_4 permeance across the composite membrane was studied. It was noticed that with increasing pressure from 5 to 15 bar caused to decreased in CH_4 permeance across the nanocomposite membrane as given in figure 28. The reasons for that are the same as discussed in above section 4.8.1.

The maximum permeance for CH_4 was noticed for pure PVA membrane i.e. 0.0131 $m^3(STP)/m^2.bar.hr$ at 5 bar and minimum for 1.5 wt.% PVA/Am-CNC i.e. 0.00365 $m^3(STP)/m^2.bar.hr$.

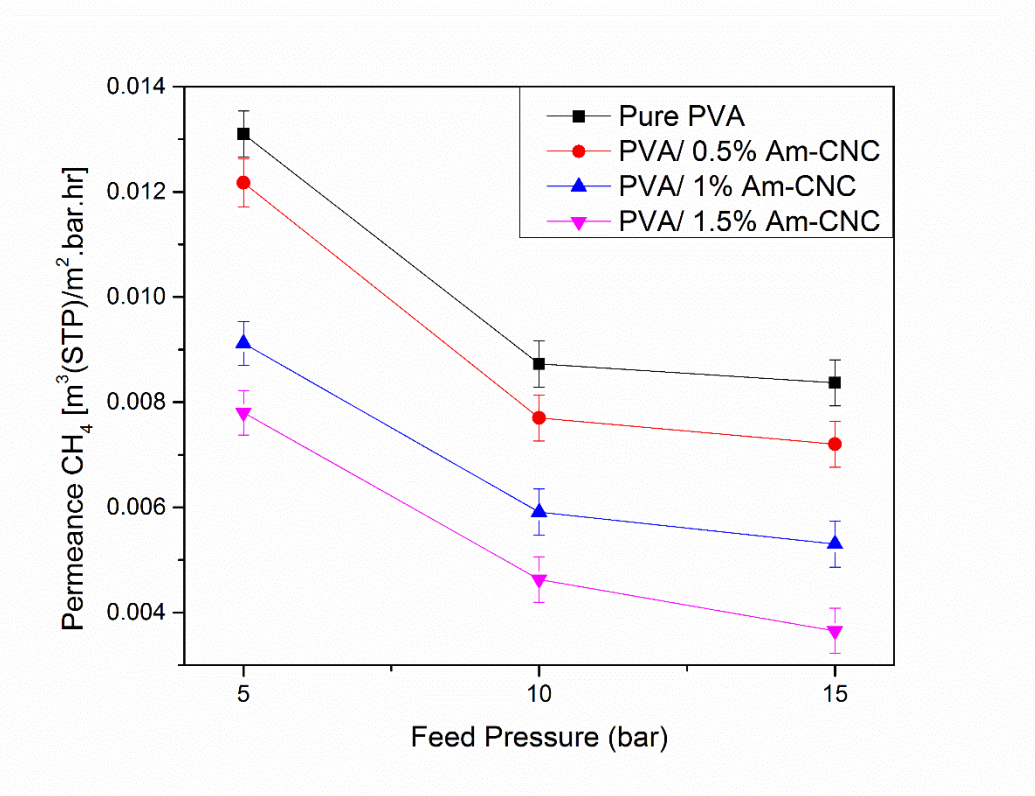

Figure 35: Effect of Pressure on CH_4 Permeance

4.8.2. Pressure Effect on Selectivity

The effect of pressure on the selectivity trend for CO_2/CH_4 is given in figure 36. The trend of selectivity is almost same as to the trend of CO_2 permeance i.e. the maximum selectivity was noticed at 5 bar pressure for 1 wt.% Am-CNC/PVA membrane is 33.55 then gradual decrease in selectivity with increasing pressure. The drop in selectivity is

because of drop in the permeance of CO_2 and CH_4 across the membrane as discussed above.

The maximum selectivity was 33.55 at 5 bar for 1 wt.% PVA/Am-CNC while minimum selectivity of 7.69 for pure PVA membrane at 15 bar was noticed [56, 90].

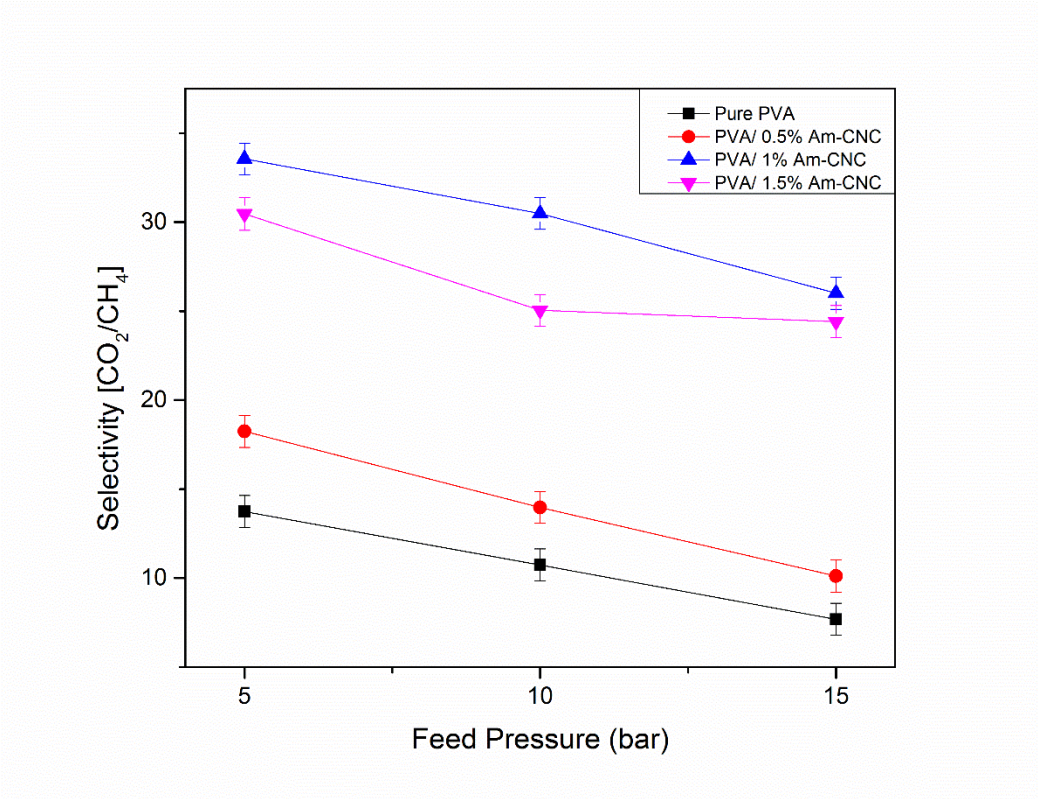

Figure 36: Pressure Effect on Selectivity

4.9. Effect of Relative Humidity

The effect of relative humidity for best membrane (1wt.% Am-CNC/PVA) at 5 bar was noticed by placing it in different humidity level i.e. 0, 25, 50, 75 and 100% respectively. The time to reached to respective humidity level was noticed from Degree of swelling graph. Figure 37(a) and 37(b) shows the effect of relative humidity on permeance and selectivity for 1wt.% Am-CNC/PVA membrane.

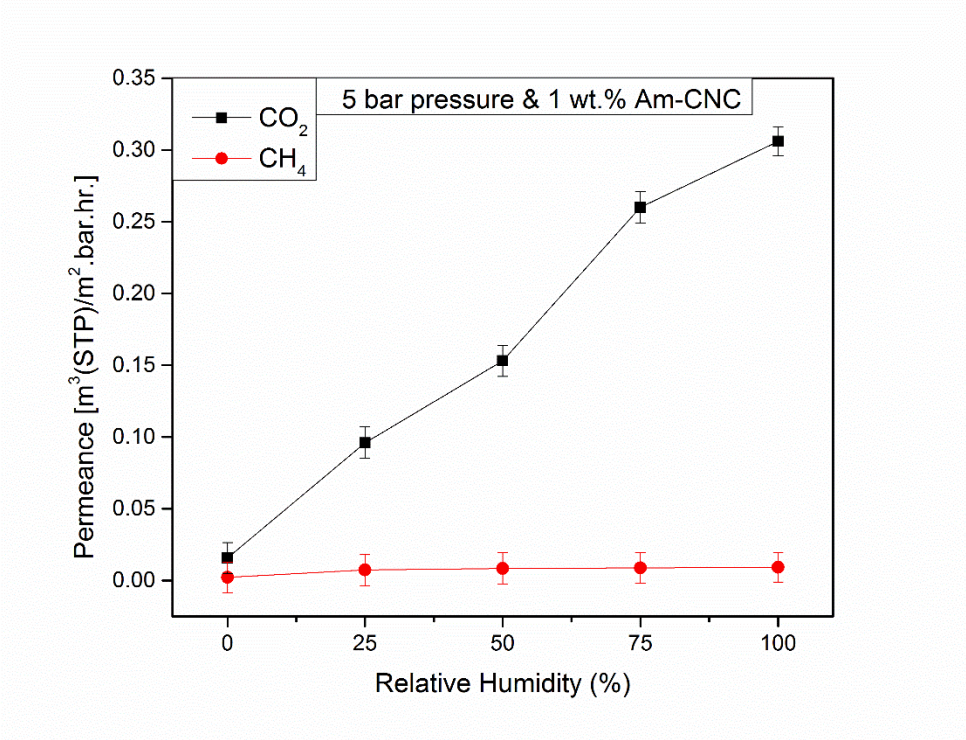

Figure 37(a): Effect of RH on permeance of CO_2 and CH_4

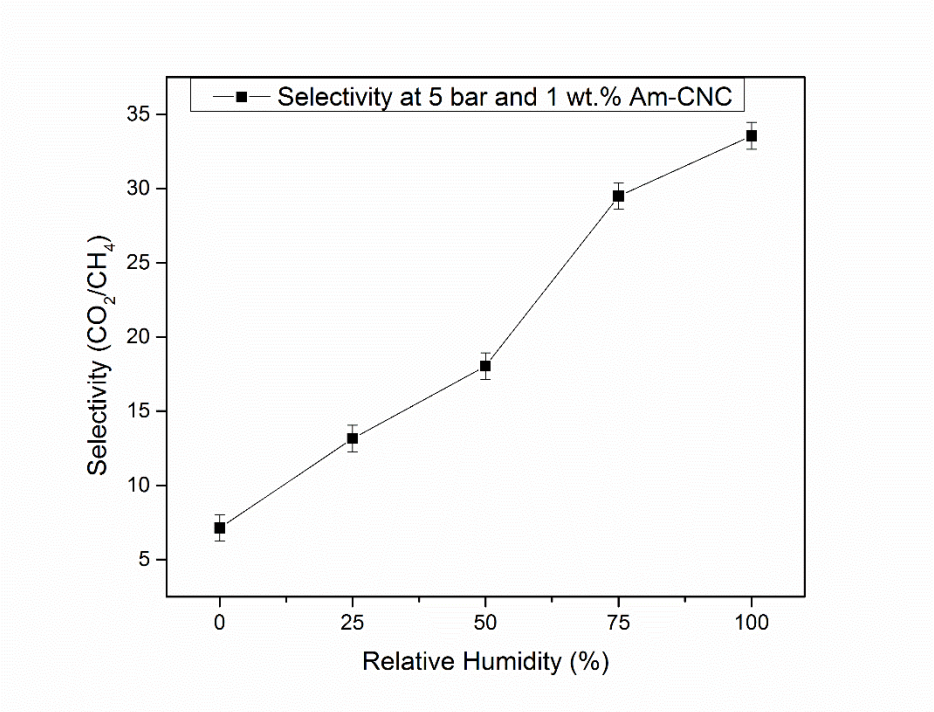

Figure 37(b): Effect of RH on selectivity

The graph shows that by increasing the RH, the CO_2 permeance and selectivity was increased. The reason for that is, by increasing the moisture uptake make to swell up the membrane. So, free volume of membrane also increased, due to which the CO_2 and CH_4 permeance also increased. The increased in moisture uptake, also increased the facilitated transport of CO_2 across the membrane. The CH_4 permeance was only due to diffusion phenomena, no facilitated transport which caused to increase the selectivity.

From figure 34(a) it was noticed that there is no effect of RH on CH_4 permeance as compared to CO_2 permeance. The table 5 shows the permeance and selectivity for 1wt.% Am-CNC/PVA at different RH;

Table 5: Relative Humidity Effect on Permeance and Selectivity

Relative Humidity	**CO_2 Permeance**	**CH_4 Permeance**	**Selectivity**
%	m^3(STP)/m^2.bar.hr	m^3(STP)/m^2.bar.hr	CO_2/CH_4
0	0.0157	0.00220	7.136
25	0.096	0.00720	13.333
50	0.153	0.00848	18.042
75	0.26	0.00881	29.511
100	0.306	0.00912	33.552

Conclusions

CO_2 removal performance for PVA/Am-CNC based facilitated transport membranes have been investigated. It was observed from the results that the separation ability of membrane was effected by increasing concentration of filler and feed pressure.

The moisture uptake performance of PVA based membrane was improved by adding Am-CNC. So, it makes Am-CNC as suitable choice to use as filler in PVA based membrane for CO_2 removal. The PVA membranes crystallinity also increased with increase in Am-CNC concentration. The membrane thickness has also increased with increasing Am-CNC concentration.

The permeability and selectivity was increased by adding filler (Am-CNC) compared to neat PVA based membranes. However; it was also noticed from the results that the separation performance of membrane increased only up to adding 1 wt.% Am-CNC (w.r.t PVA concentration) which was considered as a threshold value, after that the performance of membrane was going to decreased.

The feed pressure effect was investigated and it was noticed that the pressure has inverse relation with membrane performance. The best result was shown at 5 bar pressure, after that the performance of membranes was decreased with increasing the feed pressure. Over all, the best performance in term of permeance and selectivity was shown by PVA/1 wt.% Am-CNC based membrane.

Summary of all above discussion was following;

- Moisture uptake ability was improved by adding Am-CNC as filler in nanocomposite membrane.
- The crystallinity of nanocomposite membranes was increased by adding Am-CNC as filler.
- The thickness of dense layer over support was increased by adding Am-CNC as a filler.
- By increasing the feed pressure, decreased the performance of nanocomposite membranes.

- The best permeance result was noticed at PVA/1 wt.% Am-CNC based nanocomposite membrane.

In table 5 the literature data for the comparison of the permeance and selectivity of CO_2/CH_4 for different polymer and filler used. The experimental conditions in these data was different i.e. according to the requirement.

References

[1] I. E. Agency, "Global Energy and CO2 Status Report 2018," 2019.

[2] B. R. Singh and O. Singh, Global trends of fossil fuel reserves and climate change in the 21st century vol. 8: chapter, 2012.

[3] J. W. Tester, E. M. Drake, M. J. Driscoll, M. W. Golay, and W. A. Peters, "Sustainable Energy: Choosing Among Options. 1st," ed: MIT Press, 2005.

[4] N. Panwar, S. Kaushik, and S. Kothari, "Role of renewable energy sources in environmental protection: A review," Renewable and Sustainable Energy Reviews, vol. 15, pp. 1513-1524, 2011.

[5] P. A. Owusu and S. Asumadu-Sarkodie, "A review of renewable energy sources, sustainability issues and climate change mitigation," Cogent Engineering, vol. 3, p. 1167990, 2016.

[6] S. S. Amjid, M. Q. Bilal, M. S. Nazir, and A. Hussain, "Biogas, renewable energy resource for Pakistan," Renewable and Sustainable Energy Reviews, vol. 15, pp. 2833-2837, 2011.

[7] H. Peimani and F. Taghizadeh-Hesary, "The Role of Renewable Energy in Resolving Energy Insecurity in Asia," 2019.

[8] Y. Li, C. Alaimo, M. Kim, N. Y. Kado, J. Peppers, J. Xue, et al., "Composition and Toxicity of Biogas Produced from Different Feedstocks in California," Environmental science & technology, 2019.

[9] N. Abatzoglou and S. Boivin, "A review of biogas purification processes," Biofuels, Bioproducts and Biorefining, vol. 3, pp. 42-71, 2009.

[10] M. Banja, M. Jégard, V. Motola, and R. Sikkema, "Support for biogas in the EU electricity sector–A comparative analysis," Biomass and Bioenergy, vol. 128, p. 105313, 2019.

[11] W. b. association, "Global Potential of Biogas," 2018.

[12] Q. Sun, H. Li, J. Yan, L. Liu, Z. Yu, and X. Yu, "Selection of appropriate biogas upgrading technology-a review of biogas cleaning, upgrading and utilisation," Renewable and Sustainable Energy Reviews, vol. 51, pp. 521-532, 2015.

[13] T. Gas, "Bio Gas Updraging system."

[14] M. R. Al Mamun and S. Torii, "Removal of hydrogen sulfide (H2S) from biogas using zero-valent iron," Journal of Clean Energy Technologies, vol. 3, pp. 428-432, 2015.

[15] A. Petersson and A. WeLLInGer, "Biogas upgrading technologies–developments and innovations," IEA bioenergy, vol. 20, pp. 1-19, 2009.

[16] I. Angelidaki, L. Treu, P. Tsapekos, G. Luo, S. Campanaro, H. Wenzel, et al., "Biogas upgrading and utilization: current status and perspectives," Biotechnology advances, vol. 36, pp. 452-466, 2018.

[17] W. Baldus and D. Tillman, "Conditions which need to be fulfilled by membrane systems in order to compete with existing methods for gas separation," Membranes in Gas Separation and Enrichment, p. 2642, 1986.

[18] P. Bernardo, E. Drioli, and G. Golemme, "Membrane gas separation: a review/state of the art," Industrial & Engineering Chemistry Research, vol. 48, pp. 4638-4663, 2009.

[19] B. D. Freeman, "Basis of permeability/selectivity tradeoff relations in polymeric gas separation membranes," Macromolecules, vol. 32, pp. 375-380, 1999.

[20] L. M. Robeson, "Correlation of separation factor versus permeability for polymeric membranes," Journal of membrane science, vol. 62, pp. 165-185, 1991.

[21] T. Aoki, "Macromolecular design of permselective membranes," Progress in Polymer Science, vol. 24, pp. 951-993, 1999.

[22] M. Zaman and J. H. Lee, "Carbon capture from stationary power generation sources: A review of the current status of the technologies," Korean Journal of Chemical Engineering, vol. 30, pp. 1497-1526, 2013.

[23] K. V. Agrawal, L. W. Drahushuk, and M. S. Strano, "Observation and analysis of the Coulter effect through carbon nanotube and graphene nanopores," Philosophical Transactions of the Royal Society A: Mathematical, Physical and Engineering Sciences, vol. 374, p. 20150357, 2016.

[24] J. G. Wijmans and R. W. Baker, "The solution-diffusion model: a review," Journal of membrane science, vol. 107, pp. 1-21, 1995.

[25] D. R. Paul, "The solution-diffusion model for swollen membranes," Separation and Purification Methods, vol. 5, pp. 33-50, 1976.

[26] M. Galizia, W. S. Chi, Z. P. Smith, T. C. Merkel, R. W. Baker, and B. D. Freeman, "50th anniversary perspective: Polymers and mixed matrix membranes for gas and vapor separation: A review and prospective opportunities," Macromolecules, vol. 50, pp. 7809-7843, 2017.

[27] H. B. Park, S. H. Han, C. H. Jung, Y. M. Lee, and A. J. Hill, "Thermally rearranged (TR) polymer membranes for CO2 separation," Journal of Membrane Science, vol. 359, pp. 11-24, 2010.

[28] D. Hofmann and E. Tocci, "Molecular Modeling, A tool for the knowledge-based design of polymer-based membrane materials," in Membrane Operations, ed: Wiley Online Library, 2009, pp. 3-18.

[29] A. Javaid, "Membranes for solubility-based gas separation applications," Chemical Engineering Journal, vol. 112, pp. 219-226, 2005.

[30] P. M. Budd and N. B. McKeown, "Highly permeable polymers for gas separation membranes," Polymer Chemistry, vol. 1, pp. 63-68, 2010.

[31] C. Z. Liang, T.-S. Chung, and J.-Y. Lai, "A review of polymeric composite membranes for gas separation and energy production," Progress in Polymer Science, 2019.

[32] B. Shimekit and H. Mukhtar, "Natural gas purification technologies-major advances for CO2 separation and future directions," in Advances in natural gas technology, ed: IntechOpen, 2012.

[33] S. Doong, "Membranes, adsorbent materials and solvent-based materials for syngas and hydrogen separation," in Functional Materials for Sustainable Energy Applications, ed: Elsevier, 2012, pp. 179-216.

[34] R. Quinn, J. Appleby, and G. Pez, "New facilitated transport membranes for the separation of carbon dioxide from hydrogen and methane," Journal of Membrane Science, vol. 104, pp. 139-146, 1995.

[35] J. Mulder, Basic principles of membrane technology: Springer Science & Business Media, 2012.

[36] M. Caplow, "Kinetics of carbamate formation and breakdown," Journal of the American Chemical Society, vol. 90, pp. 6795-6803, 1968.

[37] P. Danckwerts, "The reaction of CO2 with ethanolamines," Chemical Engineering Science, vol. 34, pp. 443-446, 1979.

[38] H. Matsuyama, M. Teramoto, and H. Sakakura, "Selective permeation of CO2 through poly 2-(N, N-dimethyl) aminoethyl methacrylate membrane prepared by plasma-graft polymerization technique," Journal of Membrane Science, vol. 114, pp. 193-200, 1996.

[39] Y. Cai, Z. Wang, C. Yi, Y. Bai, J. Wang, and S. Wang, "Gas transport property of polyallylamine–poly (vinyl alcohol)/polysulfone composite membranes," Journal of Membrane Science, vol. 310, pp. 184-196, 2008.

[40] J. Goddard, "Further applications of carrier-mediated transport theory—A survey," Chemical Engineering Science, vol. 32, pp. 795-809, 1977.

[41] D. Q. Vu, W. J. Koros, and S. J. J. J. o. M. S. Miller, "Mixed matrix membranes using carbon molecular sieves: I. Preparation and experimental results," vol. 211, pp. 311-334, 2003.

[42] B. Zornoza, C. Tellez, J. Coronas, J. Gascon, F. J. M. Kapteijn, and M. Materials, "Metal organic framework based mixed matrix membranes: An increasingly important field of research with a large application potential," vol. 166, pp. 67-78, 2013.

[43] M. Gholami, T. Mohammadi, S. Mosleh, and M. J. C. P. Hemmati, "CO 2/CH 4 separation using mixed matrix membrane-based polyurethane incorporated with ZIF-8 nanoparticles," vol. 71, pp. 1839-1853, 2017.

[44] T. Yui, S. Nishimura, S. Akiba, and S. J. C. r. Hayashi, "Swelling behavior of the cellulose Iβ crystal models by molecular dynamics," vol. 341, pp. 2521-2530, 2006.

[45] L. Ansaloni, J. Salas-Gay, S. Ligi, and M. G. J. J. o. M. S. Baschetti, "Nanocellulose-based membranes for CO2 capture," vol. 522, pp. 216-225, 2017.

[46] M. Börjesson, G. J. C.-f. a. Westman, and c. trends, "Crystalline nanocellulose—preparation, modification, and properties," pp. 159-191, 2015.

[47] Y. Habibi, L. A. Lucia, and O. J. Rojas, "Cellulose nanocrystals: chemistry, self-assembly, and applications," Chemical reviews, vol. 110, pp. 3479-3500, 2010.

[48] A. Chandel and S. S. Da Silva, Sustainable Degradation of Lignocellulosic Biomass: Techniques, Applications and Commercialization: BoD–Books on Demand, 2013.

[49] F. Jiang and Y.-L. Hsieh, "Super water absorbing and shape memory nanocellulose aerogels from TEMPO-oxidized cellulose nanofibrils via cyclic freezing–thawing," Journal of Materials Chemistry A, vol. 2, pp. 350-359, 2014.

[50] M. S. Sarwar, M. B. K. Niazi, Z. Jahan, T. Ahmad, and A. Hussain, "Preparation and characterization of PVA/nanocellulose/Ag nanocomposite films for antimicrobial food packaging," Carbohydrate polymers, vol. 184, pp. 453-464, 2018.

[51] S. Beck-Candanedo, M. Roman, and D. G. J. B. Gray, "Effect of reaction conditions on the properties and behavior of wood cellulose nanocrystal suspensions," vol. 6, pp. 1048-1054, 2005.

[52] X. M. Dong, J.-F. Revol, and D. G. J. C. Gray, "Effect of microcrystallite preparation conditions on the formation of colloid crystals of cellulose," vol. 5, pp. 19-32, 1998.

[53] J. George, S. J. N. Sabapathi, science, and applications, "Cellulose nanocrystals: synthesis, functional properties, and applications," vol. 8, p. 45, 2015.

[54] Z. Jahan, M. B. K. Niazi, and Ø. W. Gregersen, "Mechanical, thermal and swelling properties of cellulose nanocrystals/PVA nanocomposites membranes," Journal of industrial and engineering chemistry, vol. 57, pp. 113-124, 2018.

[55] G. T. Rochelle, "Amine scrubbing for CO2 capture," Science, vol. 325, pp. 1652-1654, 2009.

[56] Z. Jahan, M. B. K. Niazi, M.-B. Hägg, and Ø. W. Gregersen, "Cellulose nanocrystal/PVA nanocomposite membranes for CO2/CH4 separation at high pressure," Journal of Membrane Science, vol. 554, pp. 275-281, 2018.

[57] X. Wang, Y. Zhang, S. Wang, H. Jiang, S. Liu, Y. Yao, et al., "Synthesis and characterization of amine-modified spherical nanocellulose aerogels," Journal of materials science, vol. 53, pp. 13304-13315, 2018.

[58] M. Flieger, M. Kantorova, A. Prell, T. Řezanka, and J. Votruba, "Biodegradable plastics from renewable sources," Folia microbiologica, vol. 48, p. 27, 2003.

[59] N. Li, C. Xiao, S. An, and X. Hu, "Preparation and properties of PVDF/PVA hollow fiber membranes," Desalination, vol. 250, pp. 530-537, 2010.

[60] J. H. Kim, J. Y. Kim, Y. M. Lee, and K. Y. Kim, "Properties and swelling characteristics of cross-linked poly (vinyl alcohol)/chitosan blend membrane," Journal of applied polymer science, vol. 45, pp. 1711-1717, 1992.

[61] L. Deng, T.-J. Kim, and M.-B. Hägg, "Facilitated transport of CO2 in novel PVAm/PVA blend membrane," Journal of Membrane Science, vol. 340, pp. 154-163, 2009.

[62] R. Murmu and H. Sutar, "A Novel SPEEK-PVA-TiO 2 Proton Conducting Composite Membrane for PEMFC Operations at Elevated Temperature," Journal of Polymer Materials, vol. 35, 2018.

[63] S. B. Kuila and S. K. Ray, "Dehydration of dioxane by pervaporation using filled blend membranes of polyvinyl alcohol and sodium alginate," Carbohydrate polymers, vol. 101, pp. 1154-1165, 2014.

[64] K. Ebert, D. Fritsch, J. Koll, and C. Tjahjawiguna, "Influence of inorganic fillers on the compaction behaviour of porous polymer based membranes," Journal of membrane science, vol. 233, pp. 71-78, 2004.

[65] M. Jämsä, "Improving the efficiencies of photoautotrophic biofuel production: from biomass to biocatalysts."

[66] R. Nickerson and J. Habrle, "Cellulose intercrystalline structure," Industrial & Engineering Chemistry, vol. 39, pp. 1507-1512, 1947.

[67] X. An, Y. Wen, D. Cheng, X. Zhu, and Y. Ni, "Preparation of cellulose nano-crystals through a sequential process of cellulase pretreatment and acid hydrolysis," Cellulose, vol. 23, pp. 2409-2420, 2016.

[68] P. Lu and Y.-L. Hsieh, "Preparation and properties of cellulose nanocrystals: rods, spheres, and network," Carbohydrate polymers, vol. 82, pp. 329-336, 2010.

[69] M.-J. Cho, B.-D. J. J. o. I. Park, and E. Chemistry, "Tensile and thermal properties of nanocellulose-reinforced poly (vinyl alcohol) nanocomposites," vol. 17, pp. 36-40, 2011.

[70] Z. Jahan, M. B. K. Niazi, Ø. W. J. J. o. i. Gregersen, and e. chemistry, "Mechanical, thermal and swelling properties of cellulose nanocrystals/PVA nanocomposites membranes," vol. 57, pp. 113-124, 2018.

[71] K. Singh, J. K. Arora, T. J. M. Sinha, and S. Srivastava, "Functionalization of nanocrystalline cellulose for decontamination of Cr (III) and Cr (VI) from aqueous system: computational modeling approach," Clean Technologies and Environmental Policy, vol. 16, pp. 1179-1191, 2014.

[72] L. Jin, W. Li, Q. Xu, and Q. Sun, "Amino-functionalized nanocrystalline cellulose as an adsorbent for anionic dyes," Cellulose, vol. 22, pp. 2443-2456, 2015.

[73] T. J. Kim, B. Li, and M. B. Hägg, "Novel fixed-site–carrier polyvinylamine membrane for carbon dioxide capture," Journal of Polymer Science Part B: Polymer Physics, vol. 42, pp. 4326-4336, 2004.

[74] T.-J. Kim, H. Vrålstad, M. Sandru, and M.-B. Hägg, "Separation performance of PVAm composite membrane for CO2 capture at various pH levels," Journal of membrane science, vol. 428, pp. 218-224, 2013.

[75] T.-J. Kim, M. W. Uddin, M. Sandru, and M.-B. Hägg, "The effect of contaminants on the composite membranes for CO2 separation and challenges in up-scaling of the membranes," Energy Procedia, vol. 4, pp. 737-744, 2011.

[76] M. Sandru, S. H. Haukebø, and M.-B. Hägg, "Composite hollow fiber membranes for CO2 capture," Journal of Membrane Science, vol. 346, pp. 172-186, 2010.

[77] Y. Zhang, Z. Wang, and S. Wang, "Novel fixed-carrier membranes for CO2 separation," Journal of applied polymer science, vol. 86, pp. 2222-2226, 2002.

[78] Y. Zhang, Z. Wang, and S. Wang, "Selective permeation of CO2 through new facilitated transport membranes," Desalination, vol. 145, pp. 385-388, 2002.

[79] J. Zou and W. W. Ho, "CO2-selective polymeric membranes containing amines in crosslinked poly (vinyl alcohol)," Journal of Membrane Science, vol. 286, pp. 310-321, 2006.

[80] J.-M. Hong, Y. S. Kang, J. Jang, and U. Y. Kim, "Analysis of facilitated transport in polymeric membrane with fixed site carrier 2. Series RC circuit model," Journal of membrane science, vol. 109, pp. 159-163, 1996.

[81] S. Rafiq, L. Deng, and M. B. Hägg, "Role of facilitated transport membranes and composite membranes for efficient CO2 capture–a review," ChemBioEng Reviews, vol. 3, pp. 68-85, 2016.

[82] H. Matsuyama, M. Teramoto, and K. Iwai, "Development of a new functional cation-exchange membrane and its application to facilitated transport of CO2," Journal of membrane science, vol. 93, pp. 237-244, 1994.

[83] H. Bai and W. W. Ho, "New carbon dioxide-selective membranes based on sulfonated polybenzimidazole (SPBI) copolymer matrix for fuel cell applications," Industrial & Engineering Chemistry Research, vol. 48, pp. 2344-2354, 2008.

[84] H. Matsuyama, A. Terada, T. Nakagawara, Y. Kitamura, and M. Teramoto, "Facilitated transport of CO2 through polyethylenimine/poly (vinyl alcohol) blend membrane," Journal of Membrane Science, vol. 163, pp. 221-227, 1999.

[85] L. Deng, T.-J. Kim, M. Sandru, and M.-B. Hägg, "PVA/PVAm blend FSC membrane for natural gas sweetening," in Proceedings of the 1st annual gas processing symposium, 2009, pp. 247-255.

[86] L. Deng and M.-B. Hägg, "Carbon nanotube reinforced PVAm/PVA blend FSC nanocomposite membrane for CO2/CH4 separation," International Journal of Greenhouse Gas Control, vol. 26, pp. 127-134, 2014.

[87] M. Saeed, S. Rafiq, L. H. Bergersen, and L. Deng, "Tailoring of water swollen PVA membrane for hosting carriers in CO2 facilitated transport membranes," Separation and Purification Technology, vol. 179, pp. 550-560, 2017.

[88] M. Saeed and L. Deng, "Carbon nanotube enhanced PVA-mimic enzyme membrane for post-combustion CO2 capture," International Journal of Greenhouse Gas Control, vol. 53, pp. 254-262, 2016.

[89] J. Ø. Torstensen, R. M. Helberg, L. Deng, Ø. W. Gregersen, and K. Syverud, "PVA/nanocellulose nanocomposite membranes for CO2 separation from flue gas," International Journal of Greenhouse Gas Control, vol. 81, pp. 93-102, 2019.

[90] Z. Jahan, M. B. K. Niazi, M.-B. Hagg, Ø. W. Gregersen, and A. Hussain, "Phosphorylated nanocellulose fibrils/PVA nanocomposite membranes for biogas

upgrading at higher pressure," Separation Science and Technology, pp. 1-11, 2019.

[91] J. J. Ojeda and M. Dittrich, "Fourier transform infrared spectroscopy for molecular analysis of microbial cells," in Microbial Systems Biology, ed: Springer, 2012, pp. 187-211.

[92] G. Hitkari, S. Singh, and G. Pandey, "Nanoparticles: An Emerging Weapon for Mitigation/Removal of Various Environmental Pollutants for Environmental Safety," in Emerging and Eco-Friendly Approaches for Waste Management, ed: Springer, 2019, pp. 359-395.

[93] P. Ahvenainen, I. Kontro, and K. Svedström, "Comparison of sample crystallinity determination methods by X-ray diffraction for challenging cellulose I materials," Cellulose, vol. 23, pp. 1073-1086, 2016.

[94] D. Romero Nieto, A. Lindbråthen, and M.-B. J. A. O. Hagg, "Effect of water interactions on polyvinylamine at different pHs for membrane gas separation," vol. 2, pp. 8388-8400, 2017.

[95] A. Mandal, D. J. J. o. I. Chakrabarty, and E. Chemistry, "Studies on the mechanical, thermal, morphological and barrier properties of nanocomposites based on poly (vinyl alcohol) and nanocellulose from sugarcane bagasse," vol. 20, pp. 462-473, 2014.

[96] A. Ferrer, C. Salas, and O. J. Rojas, "Physical, thermal, chemical and rheological characterization of cellulosic microfibrils and microparticles produced from soybean hulls," Industrial Crops and Products, vol. 84, pp. 337-343, 2016.

[97] C. Gebald, J. A. Wurzbacher, P. Tingaut, T. Zimmermann, and A. Steinfeld, "Amine-based nanofibrillated cellulose as adsorbent for CO2 capture from air," Environmental science & technology, vol. 45, pp. 9101-9108, 2011.

[98] C. Gebald, J. A. Wurzbacher, P. Tingaut, and A. Steinfeld, "Stability of amine-functionalized cellulose during temperature-vacuum-swing cycling for CO2 capture from air," Environmental science & technology, vol. 47, pp. 10063-10070, 2013.

[99] S. Liu, Y. Zhang, H. Jiang, X. Wang, T. Zhang, and Y. Yao, "High CO 2 adsorption by amino-modified bio-spherical cellulose nanofibres aerogels," Environmental chemistry letters, vol. 16, pp. 605-614, 2018.

[100] Z. Tong, V. K. Vakharia, M. Gasda, and W. W. Ho, "Water vapor and CO2 transport through amine-containing facilitated transport membranes," Reactive and Functional Polymers, vol. 86, pp. 111-116, 2015.